EXPERIMENTAL STUDIES ON CARRIER CONDUCTANCE RELATED PHENOMENA IN UNDOPED SEMI - INSULATING GALLIUM - ARSENIDE

BY

DNYANESHWAR APPARAO BHOGE

TH
LTP/1992/M
B469e

TH
621.31937
B 379e

LASER TECHNOLOGY PROGRAMME

INDIAN INSTITUTE OF TECHNOLOGY KANPUR

APRIL, 1992

THIS THESIS IS DEDICATED TO

MY PARENTS

EXPERIMENTAL STUDIES ON CARRIER CONDUCTANCE RELATED PHENOMENA IN UNDOPED SEMI-INSULATING GALLIUM-ARSENIDE

A Thesis submitted

In Partial Fulfilment of the Requirements

for the Degree of

MASTER OF TECHNOLOGY

TH 11347

by

DNYANESHWAR APPARAO BHOGE

to the

DEPARTMENT OF LASER TECHNOLOGY

INDIAN INSTITUTE OF TECHNOLOGY, KANPUR

April 1992

21 MAR 2002
CENTRAL LIBRARY
Acc. No. A.113497

LTP-1992-M-BHE-EXP-

POST GRADUATE OFFICE
Kanpur
Submitted on 7/4/92

CERTIFICATE

It is certified that the work contained in the thesis entitled " Experimental studies on carrier conductance related phenomena in undoped semi–insulating Gallium–Arsenide ", by *Dnyaneshwar Apparao Bhoge* has been carried out under our supervision and that this work has not been submitted elsewhere for a degree.

Dr. Y. N. MOHAPATRA
Assistant Professor
Dept. of Physics & Material Science
Indian Institute of Technology
Kanpur

Dr. R. SHARAN
Professor
Department of Electrical Engineering
Indian Institute of Technology
Kanpur

ACKNOWLEDGEMENTS

I am indebted to Dr. R. Sharan and Dr. Y. N. Mohapatra for the guidance provided by them during the course of this work. I am thankful to Dr. Y. N. Mohapatra for introducing this problem and for his interest in successful completion of this work. I am also thankful to Dr. R. Sharan for his constructive criticism during this work.

It gives me pleasure to acknowledge Sandeep Agarwal for his help and co–operation during this work. I am also thankful to him for fruitful discussions, which evolved many inventionary ideas.

I express my sincere thanks to Dr. J. Narain, Abhay Karandikar, Mrs. B. kanmani, Rajan Gurjar, Diwakar, Rahul, Gorhe, Bapat, Sidhye for the help rendered by them during this work.

I am thankful to my friends Madhav, Tatya, Wadya, Katkade, Vinya, S. Deshpande, Patil, Wajge, Mahesh Natu, Jain, and all '*patiiiil's*' *of Ghat Aisho–ciation* who made my stay at IIT enjoyful and memorable.

Finally, I would like to thank many of my friends and persons who have made my stay here an immensely educative experience.

D. A. BHOGE

CONTENTS

LIST OF FIGURES

ABSTRACT

Semi–insulating GaAs has become an important material due to its increasing importance in frontier technology, as a high voltage sub–nanosecond photo–conductive switch material, optically controlled switch and photo–refractive material apart from its use as substrate in GaAs based opto–electronic and electronic integrated circuits.

The present work is mainly devoted towards experimental studies of current transport mechanism, and investigations into the role of electrical and optical carrier injection in oscillatory conductance and defect related phenomena in semi–insulating GaAs. In this work we studied current–voltage characteristics with injecting ohmic contacts in dark and light–on conditions at room temperature. We also studied photo–induced and photocurrent transients as a function of dc electric field and photon flux.

In the present work we observe that, the current transport mechanism is a complex behaviour involving interaction between carrier injection and trapping & detrapping of carriers by deep level traps. We observe a close relationship between current–voltage characteristics and the oscillatory behaviour. The oscillatory phenomena in semi–insulating GaAs is shown to be governed by degree of sublinearity in the current–voltage characteristics. We observe that, the time constants of photo–induced transients involve activation energies different from that of dominant donor EL2 in these materials and may possibly involve emission from 0.56 eV and 0.4 eV deep level traps and/or Poole–Frenkel emission from these traps due to high field near one of the contacts. We observe that, the critical parameter for the onset of decaying oscillations in current transients is the density of carriers inside the device.

CHAPTER 1

INTRODUCTION

1.1 INTRODUCTORY VIEW :

A variety of integrated circuits and devices have now been developed. Depending upon the desired characteristic of the device, different semiconducting materials are utilised; dominant among these are silicon and III–V semiconductors.

Among the various III – V compounds, GaAs turned out to be an excellent material for high performance applications because of its direct wide energy bandgap, high electron mobility and availability of semi–insulating (SI) GaAs substrate. Several devices have been developed using GaAs and many of these utilise a semi–insulating substrate.

Semi–insulating GaAs has resistivity of the order of 10^7– 10^8 Ω cm . Semi–insulating property is obtained by overcompensating the shallow impurities by deep impurities of opposite type. Semi–insulating GaAs substrate offers a natural isolation between the active devices preventing undesirable effects such as sidegating etc.

In the beginning GaAs based IC technology faced major problem of fabrication of high quality substrate. Earlier attempt for preparation of SI–GaAs was to use Cr–doping, but the high solid state diffusivity and anomalous surface aggregation of chromium led to problems of conversion of surface layer. This was affecting the device properties such as peak channel current and threshold voltage. Historically, Cr–doped SI–GaAs was first grown by either a modified horizontal bridgeman technique or by gradient freeze.

The problem of obtaining SI–GaAs was solved with the development of the Liquid Encapsulation Czochralski (LEC)[7–8] technique which adopted the simple solution of covering the GaAs melt with a layer of inert molten glass – boric oxide. It is known that in LEC grown undoped SI–GaAs material shallow as well as deep level impurities are present. The shallow

donor impurities are Si and S on gallium and arsenic site respectively and shallow acceptor C on arsenic site[9–10]. The most important deep level donor impurity present is the so–called EL2 electron trap. The origin of EL2 trap is believed to be related to the native Arsenic anti–site (As_{Ga}) defect[11]. This EL2 electron trap plays major role in obtaining semi–insulating property. In undoped LEC grown GaAs crystal the shallow acceptor concentration is in excess of the shallow donor concentration. The semi–insulating property of LEC grown GaAs is because of compensation of shallow acceptor C by the deep donor EL2 trap.

The conventional methods such as Hall resistivity and capacitance measurement techniques used for characterisation of semiconductors, are not suitable for characterising high resistivity materials. The use of Hall resistivity method led to the problems of low signal to noise ratio and also the capacitance technique is not practicable. Many investigators have found that the methods such as thermally stimulated conductivity (TSC)[6], space charge limited conductivity[6,22,23], photo–induced current transient spectra technique[14–21] are suitable for characterising the deep levels in high resistivity materials.

After studies on deep donor trap EL2 in SI–GaAs by G. M. Martin et al[10], many investigators have shown that the EL2 impurity plays very important role in the observable phenomena such as low frequency current oscillations[29–38] and photoconductive switching behaviour[40–44]. Semi–insulating GaAs is still under intensive research due to its increasing importance in frontier technology as a high voltage photo–conductive switch material, optically controlled switch material with silicon doping and photo–refractive device apart from its use as substrate in GaAs based integrated circuits.

For the first time D.C. Northrop[29] observed low frequency oscillation phenomena in high resistivity GaAs. These oscillations are different from the Gunn oscillations, which are due to the high field domain formation and the travel caused by a transfer of hot electrons from a high mobility central valley to a low mobility secondury minimum in the conduction band. The low frequency oscillations are believed to be due to formation of high field domains and the travel caused by field enhanced capture of electrons from the conduction band to

a trap state[39]. The frequency of these oscillations lie in the range of few Hz to a few kHz, depending on the temperature, illumination and the electric field[31,33,34,37,39]. Although many features of low frequency oscillations are studied experimentally, inorder to model this phenomena there exists no direct experimental evidence of dc field dependence of capture cross section of deep level traps. One of the theme of the present work is experimental investigation of dc field dependence of capture cross section of deep level EL2 trap. Many people have tried to model this phenomena, but there is no satisfactory explanation to various facets of this phenomena.

Due to increasing importance of semi–insulating GaAs in frontier technology it is important to understand current transport mechanism in SI–GaAs. Many workers have studied current–voltage (I–V) characteristic and observed that the semi–insulating GaAs material shows different regimes of conduction mechanism. The work carried out sofar is not sufficient to understand conduction mechanism in SI–GaAs. Recentaly Grischowsky et al [25] viewed semi–insulating GaAs with two planar ohmic contacts as a metal–semiinsulator–metal (M–SI–M) structure. This M–SI–M structure forms an excellent device for studying the carrier injection mechanism in the study of current conduction mechanism in semi–insulating GaAs.

The present work is mainly devoted towards the experimental study of current conduction mechanism and investigation of oscillatory phenomena in semi–insulating GaAs. In the present work we studied current–voltage characteristics of semi–insulating GaAs with injecting ohmic contacts. The current–voltage characteristics are studied with changing polarity of contacts in dark and light on conditions at room temperature. We studied the photo–induced and photo–current transient as a function of dc field and photon flux. In this work we studied the role and implications of electrical and optical carrier injection in semi–insulating GaAs related phenomena.

1.2 SEMI–INSULATING GAALLIUM–ARSENIDE (SI–GaAs):

1.2.1 MATERIAL PREPARATION METHODS REVIEW:

Earlier development of GaAs based IC technology faced major problem o preperation of high quality semi–insulating substrate. The following paragraph will outline th methods of preperation of SI–GaAs substrate. Earlier attempt of preparing SI–GaAs used th following technique.

1. Horizontal bridgeman growth technique.
2. Vertical gradient freeze technique.

These methods made use of silica boats or crucibles for synthesizing GaAs. This led to a singl crystal with very high silicon impurity content ($>10^{16}$ cm^{-3}) (located predominantly on the dono site Si_{Ga}). To obtain semi–insulating behaviour these methods made use of high level o Cr–doping. The Cr impurity forms a deep acceptor level which compensate the Si shallow donor Due to high solid state diffusivity and anomalous surface aggregation of chromium, such material led to problems of conversion of surface layer affecting the device parameters such as peak channe current and threshold voltage.

The problem of obtaining high quality semi–insulating substrate got solved wit the development of Liquid Encapsulation Czochralski (LEC)method[7–8]. This method used simpl solution of covering the GaAs melt with a layer of an inert molten glass– boric oxide. This metho produced material which is either nearly stoichiometric or As–rich. The SI property of undope material derives from a native defect EL2 donor, the concentration of which is related t stoichiometry. This EL2 deep donor compensate the shallow impurities.

1.2.2 PROPERTIES OF SI–GaAs:

Semi–Insulating GaAs is a III–V compound direct bandgap semiconduct material. It can be obtained in semi–insulating form. As any semiconductor has shallow ar

deep impurities, SI–GaAs material also has shallow and deep donors as well as acceptor impurities. The semi–insulating behaviour is obtained by over compensating the dominant shallow dopants with deep centers of opposite type.

If we denote the concentration of shallow acceptors by N_{a1}, the concentration of deep acceptors by N_{a2}, the total donor concentration by N_d, and the free electrons and holes concentration by n & p respectively, then material is semi–insulating when

$$N_{a1} < N_d < N_{a1} + N_{a2} \qquad \text{with } \frac{n}{p} < 1 ,$$

Similarly if the condition

$$N_{d1} < N_a < N_{d1} + N_{d2} \qquad \text{with } \frac{n}{p} > 1, \text{ is filled}$$

the material is semi–insulating,

For SI–GaAs, the electrical conductivity in dark is about $3 \times 10^{-9}\ \Omega^{-1}\ cm^{-1}$, and free electron and hole densities are about $2.25 \times 10^{6}\ cm^{-3}$ at 300 k.

Also the necessary condition for obtaining SI property is that the fermi energy should be at the middle of the energy gap. This material has resistivity close to insulator value. But since this high resistivity GaAs carries electronic current, it is preferred to call it as a semi–insulator.

1.2.3 IMPURITIES AND NATIVE DEFECTS IN SI–GaAs :

In SI–GaAs different shallow and deep level impurities are present. These impurities play imporyant role in obtaining semi–insulating property. In this subsection the summery of shallow and deep impurities present in SI–GaAs material is given.

Shallow Impurities: The most important shallow impurities in SI–GaAs crystals are shallow donors Si and S on Gallium and Arsenic site respectively, with energy level about 6 meV below the conduction band and shallow acceptor C on Arsenic site with energy level about 23 meV above the

valence band with concentration about 5 x 10^{15} to 10^{16} cm^{-3} (Here the Si is an amphotoric impurity which can also play a role of a shallow acceptor when it substitutes for an arsenic atom).

If the concentrtion of residual shallow donors (S , Si) exceeds C concentration n–type material is obtained. On the otherhand if C exceeds the total donor concentration p type material is obtained.

Deep Acceptor: The well known deep acceptor present in SI–GaAs is Cr on Ga sites with energy level 0.324 eV above the valance band.

Deep donor (EL2 electron trap): This trap is investigated by Martin et al[11] using DLTS technique. In bulk SI–GaAs material the deep donor impurity observed at 0.82eV below the conduction band is denoted as EL2. The origin of this deep level trap is not yet clear. it is assumed that this trap is related to As antisite (As_{Ga}) i. e. where As is replaced by Ga. This antisite As_{Ga}defect is formed during the post growth cooling of the crystal.and its concentration depends on the melt stoichiometry.The conc. of EL2 trap is about 4 x 10^{16} cm^{-3}.

In undoped LEC GaAs crystal the shallow acceptor concentration is in excess of shallow donor level concentration ,so that the material is p type. The deep level EL2 donor concentration exceeds the net acceptor concentration so that this level pins the fermi–level close to mid gap yielding resistivities > 10^{8} ohm cm. In LEC grown undoped SI–GaAs material the shallow impurity carbon is overcompensated by deep EL2 donor.

1.2.4 TECHNOLOGICAL IMPORTANCE OF SI–GaAs Material:

Importance of EL2 trap: EL2 deep donor with an activation energy of 0.82 eV is the dominant deep level trap in LEC grown SI–GaAs . This deep level has been a subject of extensive studies for several years because of its unique physical properties as well as its unique crucial role in producing " Undoped " SI–GaAs by compensation of residdual shallow acceptors. therefore the understanding of the EL2 and its behaviour is critical for IC technology. EL2 electron trap plays a very important role in SI–GaAs related phenomenas such as low frequency oscillations, photoconductive switch behaviour.

Low frequency oscillations phenomena observed in bulk material shows that one can use the SI–GaAs material as a natural device for low frequency generator(few Hz to about 3 kHz). Semi–insulating GaAs is curently used as a substrate material for GaAs based opto–electronic devices, detectors, digital and microwave devices and intigrated circuits. Recent studies have shown that SI–GaAs is coming out to be a remarcable sub–nanosecond high power photoconductive switch material. The advantage of using SI–GaAs in a high power switch instead of Si are

a).It has a higher elecron mobility.

b).Higher dark resistance.

c).Higher dielectric strength.

d).faster recombination time.

Also the compensated silicon doped GaAs can be utilised as a material for optically controlled closing and opening switches.

1.3 ORGANISATION OF PRESENT WORK

The present work is organised in four chapters. The chapter 1 gives the introductory view along with plan of the work. Section 1.2 discusses briefly about the material preperation, properties of semi–insulating GaAs, defects present in undoped SI–GaAs and technological importance of SI–GaAs and EL2 trap.

The chapter 2 gives theoretical concepts needed in the discussion of our experimental results. Section 2.1 contains single carrier space charge limited transport mechanism in high resistivity materials. Section 2.2 summarises about the low frequency oscillations in SI–GaAs. Section 2.3 is a brief review of phenomenology of traps, experimental methods of detection and the equations governing trap parameters along with field dependence of capture and emiossin processes.

In chapter 3 we report the measurement details, observations and discussion of present work. Section 3.1 discusses briefly about the general experimental set–up along with the

advantages of present measurement technique. In section 3.2 we report sample specifications, details of measurement carried out and observations. In this section we discussed qualitatively the results observed.

Chapter 4 summarises the conclusion of the present work. This also dicusses briefly about the future scope of the present work and the problem.

CHAPTER 2

THEORETICAL ASPECT WITH LITERATURE SURVEY

2.1 SINGLE CARRIER SPACE CHARGE LIMITED CURRENT TRANSPORT:

Insulating materials show wide range of conduction mechanisms and current–voltage characteristic. One of the significant features are the injection currents. Due to the fact that the density of thermal carriers IS small in insulating materials, injected carrier density becomes significient. The presense of traps leads to wide range of behaviour. In around 1940 Mott and Gurney made the observation that metal vaccum and metal insulator contacts are very similar. Carriers will be injected from the metal into the insulator and consequentally even at room temperature there may be a sufficient number of electrons available. In the following paragraph we discuss various regimes of current–voltage characteristic.

For simplicity, the assumptions made here are,

a) Conduction is primarely due to drift.

b) Injected carriers are of one type only.

c) Density of thermal carriers is small.

d) Mobility is independent of field.

Trap free insulator :

According to simplified single carrier theory, at lower voltage the conduction is ohmic given by

$$J = \sigma_0 V/L \qquad 2.1$$

where J is the current density, σ_0 the conductiivity, V the applied voltage and L the sample thickness.

In trap free insulator the space charge limit region conduction is described by the Mott–Gurney law[2]

$$J = \frac{9}{8} \mu_n \epsilon \frac{V^2}{L^3} \qquad 2.2$$

where μ is the microscopic mobility, ϵ is the permitivity of material.

Insulator in presence of traps:

Injection under the presence of traps leads to capture of carriers by the empty traps , hence the free carriers available for conduction reduces. The total trapped carrier density is given by

$$n_t = \frac{N_t}{1 + (g)\ \mathrm{Exp}\ [(E_t - E_f)/kT]} \qquad 2.3$$

where g is the ground state degeneracy, N_t is the total trap density.

In presence of traps, the space charge limit conduction is given by Mott–Gurney law modified due to traps

$$J = \frac{9}{8} \otimes \mu_n \epsilon \frac{V^2}{L^3} \qquad 2.4$$

where $\otimes$ is the ratio of free to the shallow trapped charge.

For deep trapping however as the fermi level approaches trap level there is a suddden rise of free carrier and a sharp increase in current.

Fig.2.1 shows one carrier space charge limited current–voltage characteristic for insulator with a single trap level, in which V_{tr1} for the trap free case occurs when the transit time of the carriers becomes less than the dielectric relaxation time and

$$V_{tr1} = q\, n_o \frac{L^2}{\epsilon} \qquad 2.5$$

and V_{tr2} is the transition voltage modified due to trapping of charge in the shallow impurities.

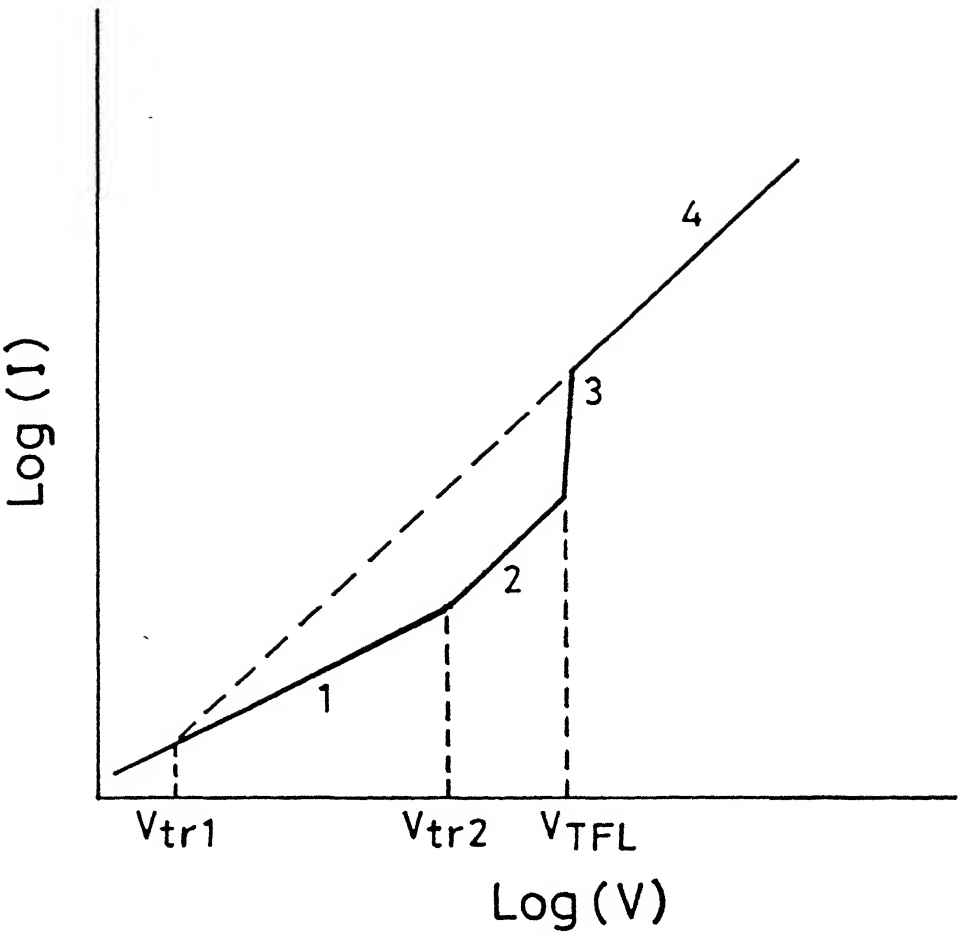

Fig.2.1 One carrier space charge limited current–voltage characteristic of insulator with a single trap level. (1) Ohm's law. (2) Modified Mott and Gurney law due to traps. (3) Trap–filled limit region. (4) Trap free Mott and Gurney law.

Effectively by noting that this can be also seen as an increase in the transit time by the factor ⊗, we have

$$\tau_{tr} = \frac{L^2}{\mu_n V_{tr} \otimes} \quad \text{and} \quad \tau_0 = \frac{\epsilon}{n_0 q \mu_n} \qquad 2.6$$

when $\tau_{tr} = \tau_0$

$$V_{tr2} = \frac{q n_0 L^2}{\epsilon \otimes} \qquad 2.7$$

The sharp increase in current when trap gets filled is due to the fact that now all additional injected charge is available as free carriers for conduction. The volTage at which current rises sharply is called trap filled limit voltage and is given by

$$V_{TFL} = \frac{q N_t}{\epsilon} L^2 \qquad 2.8$$

Valuable information about the current transport mechanism in semi–insulating GaAs can be obtained by analysing current–voltage characteristic with injecting ohmic contacts.

Recent work on I–V characteristic by different investigators shows different regimes. The current–voltage characteristic of SI–GaAs at 300^0 K in dark so far reported by many workers can be grouped into two curves as shown in fig.2.2. These characteristic shows different regimes of interest.

1. R1 corresponds to the ohmic region($I \alpha V$).
2. R2 corresponds to the transition region.
3. R3 corresponds to space charge limit (SCL) region where current is given by Mott and Gurney law ($I \alpha V^2$)modified due to traps[4,14,17–19,21,24].
4. R4 corresponds to Mott and Gurney law ($I \alpha V^2$)in trap free case[4,18,24].
5. R5 corresponds to the differential negative conductivity region where one observes low frequency

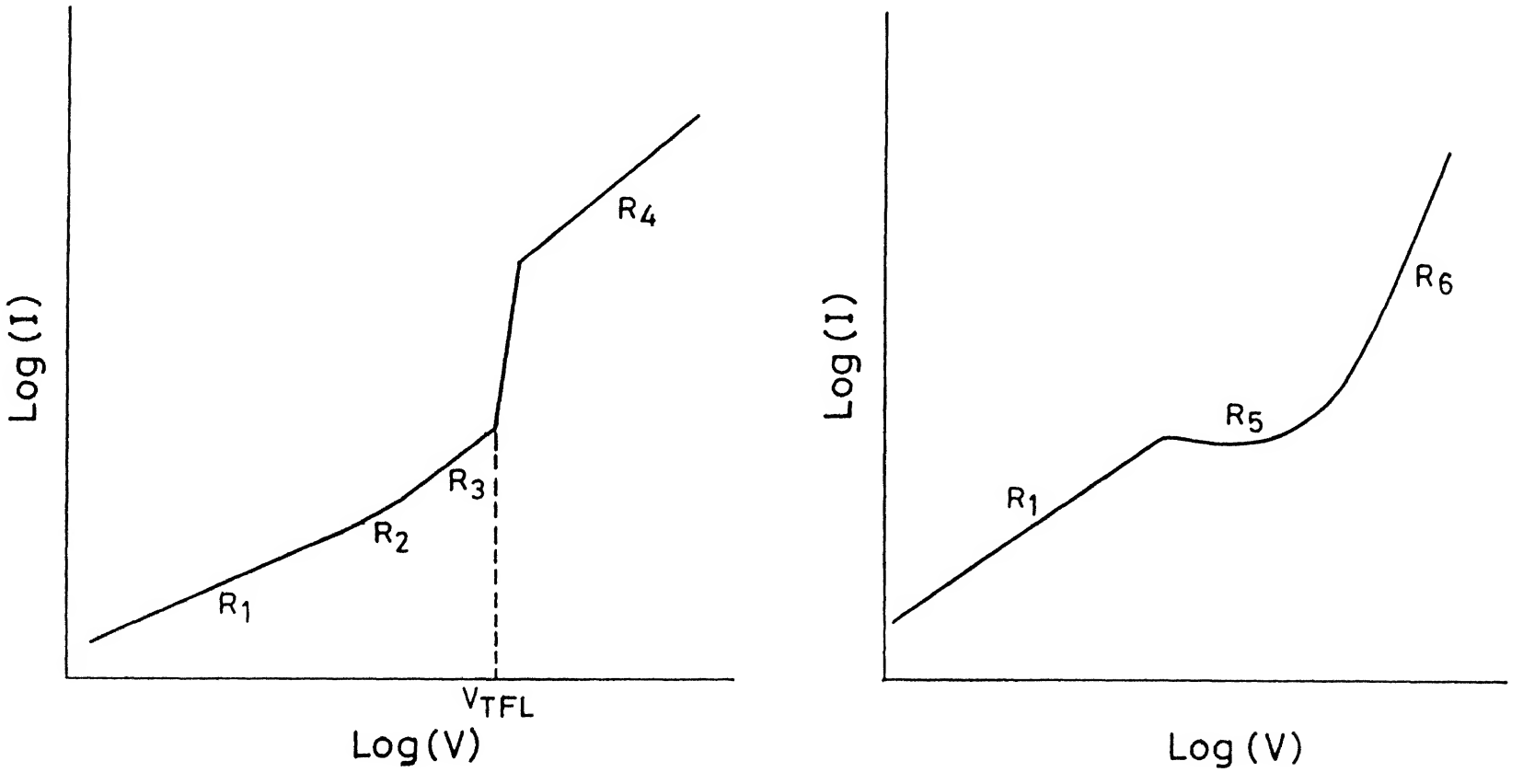

Fig.2.2 Current–voltage characteristics showing different regimes observed so far by different investigators in different samples of semi–insulating GaAs.

oscillations[5–10,22–24].

6. R6 corresponds to the double carrier injection region where $I \propto V^3$ [4.24].

the very existence of so many regimes in different samples shows how complex can be the transport mechanism in SI–GaAs.

2.1 LOW FREQUENCY OSCILLATIONS IN SI–GaAs.

In this section we briefly discuss about the low frequency oscillations in SI–GaAs and the work carried out by different workers and the models proposed.

In a semiconductor which posses voltage controlled negative differential conductivity, high field domains can build up and propogate leading to current oscillations. The best known example is Gunn oscillations in low resistivity GaAs, which are due to the high field domain formation and travel caused by a transfer of hot electrons from a high mobility central valley to a low mobility secondary minimum in the conduction band[28]. Gunn oscillation frequency lies in the MHz region.

Another type of oscillation is observed in low resistivity GaAs, which are belived to be due to high field domain formation and travel caused by field enhanced capture of electrons from the conduction band to a trap state[31]. Ridley (1966) has shown that, a semiconductor may possess a bulk differential negative resistance, if it has a deep impurity with an electron capture coefficient that increases with electric field . Fig..2.3 is a graph of current density against applied voltage showing negative differential conductivity. A material that possess a voltage controlled differential negative resistance may be expected to develop high and low field regions (Ridley 1963) and the domains so formed propogate between the contacts. The average J – V characteristics observed for the material flattens and drops with the onset of domain action instead of following a V^2 relationship as in the space charge limited flow. The domain formed travels at a velocity which is a function of the emission and the capture rate of the impurity level, and is usually in the range of 1 to 100 cm/sec, corresponding to oscillation frequency of 10 to 10^3 Hz, for a device of typical length 10^{-1} cms.

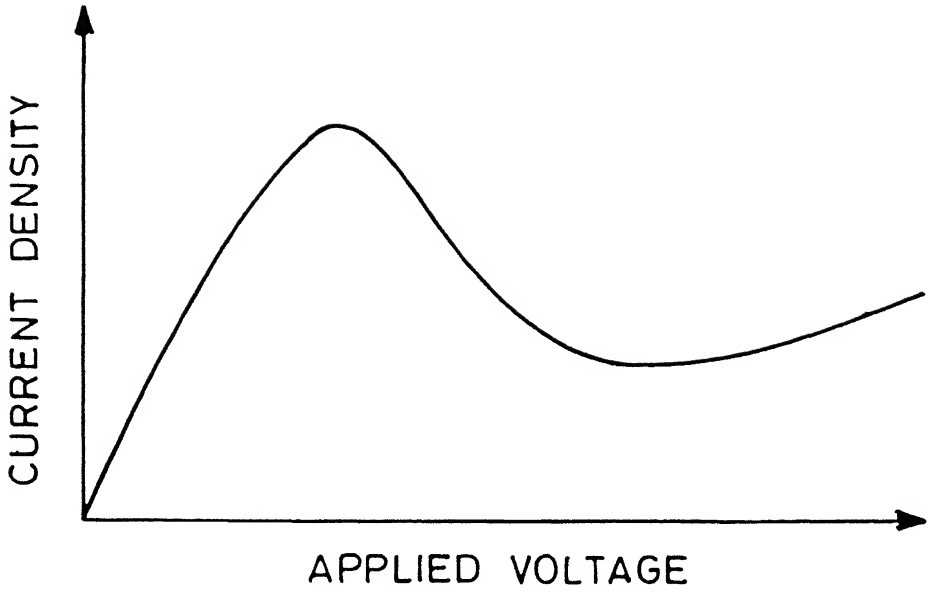

Fig.2.3 Graph of current density X applied voltage showing negative differentialconductivity.

Low frequency current oscillations in SI–GaAs have been observed for many years and various explanations as to their origin have been published[29–33]. In 1964 first time Northrop et al [29] observed low frequency oscillations in high resistivity GaAs. In 1965 Ridley and pratt also reported LFOs in SI–GaAs. The model proposed by Northrop et al is based on an analysis of dynamic equilibrium of carriers under the influence of an external field and trapping by a defect. They paid attention towards the mechanism of extraction of holes by cathode. In 1965 Ridley and Pratt proposed model based on domain formation and travel caused by trapping and detrapping of carriers by deep traps. In 1970 Sacks and Milnes[30] numerically modelled the kinetics of domain formation governed by field enhanced electron capture by deep level trap. In 1982 M. Kaminska et al[31] proposed model in which they relate the LFOs to carriers being trapped and released by the mid gap trap EL2. For oscillation to occur, the capture rate increases for hot electron, which is explained in terms of a configurational barrier, which is more easily penetrated by higher energy electrons. In 1984 H.Goronkin et al[32] proposed model based on recapture at the trailing edge of the domain, which moves with the majority carriers and causes LFOs. In 1985 G. N. Maracas[33] proposed model based on diffusion of holes for onset of LFOs.

The low frequency oscillations are functions of many parameters such as dc electric field, intensity of optical illumination and temperature. Many workers have studied the role of cathode contacts in the onset of low frequency oscillations and observed that the cathode injecting property plays important role[37–38]. At present there is no single model which satisfactorily explains various facets of this phenomena. Also, there is no direct experimental evidence of dc field dependence of capture cross section of deep level trap. One theme of present work is experimental investigation of dc field dependence of capture cross section of deep level trap so as to provide basic information in the modelling of LFO phenomena.

Positive differential resistanece region oscillations: In this paragraph we outline the principle involved in the current oscillations observed in the positive differential resistence region of current–voltage characteristics. These oscillations have been observed in semiconductors in the presence of deep impurity levels. Konstantinov[49] proposed model based on the formation of

recombination waves which may propogate through a semiconductor through which dc current is flowing. Konstantinov[49] has shown that, if the rates of electron and hole capture by deep level traps are quite different, longitudinal different waves, which may be called recombination waves, may propogate in the presence of dc current. For sufficiently high minority carrier concentrations and sufficiently strong electric fields these waves may be self excited. The details of origin of formation of recombination wave has been discussed in Ref.(49).

2.3 PHENOMENOLOGY OF TRAPS:

TRAPS AND RECOMBINATION CENTRES: In this basic concepts of traps are summarised, so as to understand trap related effects.

Those regions of the crystal which are able to capture electrons or holes, and detain them in a restricted volume are called traps. Trapping is a fundamental process for enegy storage in almost electronically active solids. This energy storage is accomplished by the spatial localisation of an excited electrons holes, in such a way that the electron or the hole is prohibited from moving freely through the crystal unless supplied with thermal or optical energy. When the trapped electron or hole is released, it is free to move until captured by a recombination center or by another trap.

A deep impurity in a semiconductor may act either as a trap or as a recombination center, depending on the impurity, on the temperature and on the various other doping conditions. Consider a majority carrier captured at an impurity center. If a carrier lives a mean life time in the captured state and is ejected thermally to the band from which it came, we may regard the center as a trap. If however, before thermal ejection can occur, a majority carrier is trapped, recombination will have taken place, and the impurity will act as a recombination center. Which role a center will play depends on the concentration of the minority carriers and on the relative crosssection for capture of minority and majority carriers.

DETECTION OF TRAPS: The following measurements are useful in

giving information about trapping. In this section, qualitatively the exprriments and information about the traps that is obtained from these is given.

Photoconductivity after beginning of excitation: If a completely deexcited material i.e. one in which the trap has been emptied by previuos heating or optical radiation, is exposed to exciting radiation, a certain proportion of the free carrier initially excited will be captured by the traps. Thus the initial density of the free carriers,and hence the initial rate of recombination between free carriers and impurity centers, is less than that which is set up in the steady state after excitation for a sufficient period of time. The information about, density of traps, capture cross sectomn can be obtained from this experiment.

Conductivity transients after cessation of excitation: Those traps which have been filled during the excitation of the material will become empty when the excitation is removed, at a rate depending on their capture crosssection and ionisation energy. Depending on the experimental conditions and the nature of the traps the curve may decay or rise exponentially. By this experiment, information about trap emmission rate, activation energy, nature of trap can be obtained.

Optically stimulated trap emptying: Filled traps may be emptied by the absorption of optical energy as well as by the utilisation of the thermal energy. Traps depths may be obtained from the stimulation spectrum of photoconductivity.

Space charge limited current dependance on voltage: Measurement of the variation of space charge limited current injected into a crystal through an ohmic contact, as a function of electric field applied to the crystal, can also be used to give an indication of the total trap density, trap distribution with energy, and hence actual location of fairly monoenergetic trapping levels.

The basic equations which summarise trap phenomenology are discussed below. In the experiment of photocinductivity measurement after cessation of light pulse , the time rate of change of free carriers n (electrons) is given by

$$\frac{dn}{dt} = e_n N_{te} - C_n n N_{ti} \qquad 2.11$$

where e_n and C_n are emission and capture coefficient. N_{te} and N_{ti} are density of trapped electrons and density of ionised traps.

In this case we neglect the radiative and Auger recombination processes. Electron emmission depends on the concentration of the trap centers occupied by electrons and the emmission rate through the relation $= e_n N_{te}$. This relationship does not contain n because it is not necessary for their to be electrons in the conduction band during the emmission process, but there must be trap centers occupied by electrons. The capture process is slightly more complicated because it depends on n and N_{ti} , and the capture coefficient C_n through the relation $= C_n n N_{ti}$. The electron concentration n is important because to capture electrons there must be electrons in the conduction band.

The relationship between emission coefficient and capture ccoefficient for electrons is given by,

$$e_n = C_n N_c \exp\left(-\frac{E_n}{kT}\right) \qquad 2.12$$

where C_n is capture coefficient defined by,

$$C_n = \sigma_n V_{th} \qquad 2.13$$

Where V_{th} is the thermal velocity of carriers, σ_n is the electron capture cross section.

The equation 2.12 can also be written as,

$$e_n = A T^2 \exp\left(-\frac{E_n}{kT}\right) \qquad 2.14$$

A is material related parameter involving electronic concentration, velocity, and emission cross section and E_n is the activation energy for the trap.

2.3.1 CAPTURE CROSS SECTION

DEFINITION: The capture cross section of the center is determined by the potential variation in the neighbourhood of the center. The largest capture cross section occur for charge centers which exert a coulomb attraction on the free carriers. Under the assumption that a free carrier will be captured if it approaches sufficiently close to a center so that the binding energy due to Coulomb attraction is equal to or greater than kT_0, a simple estimate of the corresponding value of σ can be made.

$$\sigma = \pi r^2 = \frac{10^{-10}}{\epsilon^2} \text{ cm}^2 \qquad 2.9$$

at room temperature.

For a dielectric constant ϵ of about 10, a maximum value of σ is about 10^{-12} cm^2. The normal value of σ for an uncharged center is about the order of atomic dimensions or 10^{-15} cm^2. It is possible, however, for a center actually to exert a Coulomb repulsion for free carriers, such a center will have very small capture cross secton. The smallest value of σ indicated by eperiments are aboout 10^{-22} cms^2.

2.3.2 FIELD DEPENDENCE OF EMISSION AND CAPTURE COEFFICIENT:

The Poole–Frenkel effect : This gives an idea of effect of electric field on the emission of a carrier from neutral trap. This effect results from the lowering of a coulombic potential barrier by the electric field applied to a semiconductor. For a trap to experience the effect it must be neutral when filled and posetive when empty. This effect is given in fig. 2.4. An electron energy band diagram at zero electric field is shown by the dashed lines. An energy diagram at zero electric field is shown by solid lines. An energy E_C–E_T iss required for electron emission. The bands are slanted with an applied electric field, as shown by thesolid lines, and the emission energy is reduced by ΔE. Poole–Frenkel emission over the lowered barrier is shown. The electric field required to observe this

effect is greater than 10^4–10^5 V/cm.

The barrier lowering is given by ,

$$\Delta\phi_{pf} = \left(\frac{e^3 E}{\pi \epsilon}\right)^{1/2} = \beta_{pf} E^{1/2} \quad 2.10$$

Capture coefficient field dependence: Sacks and Milnes[4] gives the idea of capture coefficient dependence on the field. A negatively charged impurity is surrounded by a potential barrier of height ϕ as shown in fig.2.5. For an electron in the conduction band to be captured by this center it must either go over the barrier or tunnel through it.

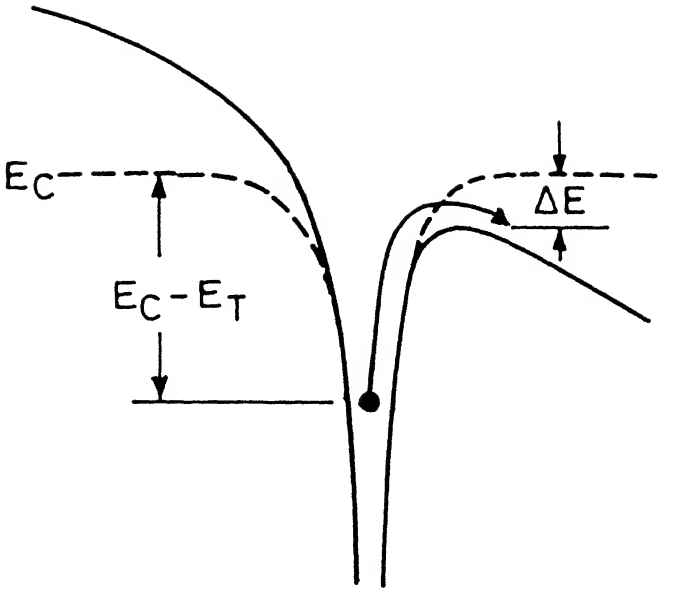

Fig.2.4 Poole–Frenkel effect.

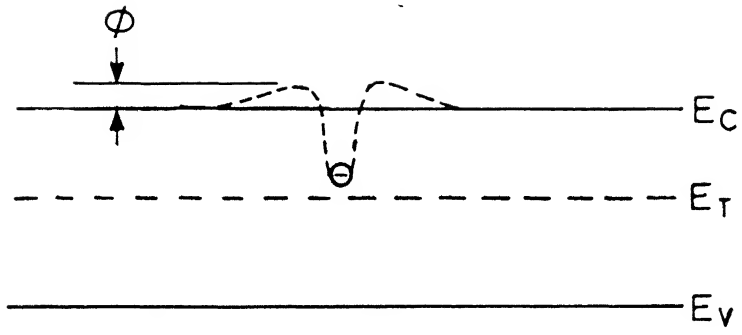

Fig.2.5 Electrostatic potential in the neighbourhood of negative charged impurity

CHAPTER 3

EXPERIMENTAL SET–UP, MEASUREMENT DETAILS, OBSERVATIONS AND DISCUSSION

In the present work our main interest is to study current conduction mechanism and the oscillatory phenomena in semi–insulating GaAs. During the study we have carried out the following measurements:

1. Current – Voltage (I–V) characteristic measurement in dark and light illumination conditions.
2. Photo–induced current transient (PICT) measurements with varying dc electric field.
3. Photocurrent transient (PCT) measurements with varying dc electric field.
4. Photocurrent transient measurements with varying photon flux.

All these measurements are carried out at room temperature.

3.1 EXPRIMENTAL SET–UP COMMON TO ALL MEASUREMENTS:

The details of the experimental conditions for each of these measurements are given in the concerned section. The following two paragraphs descibe the overall schematic set–up which is shown in fig 3.1. The monochromatic light of wavelength 6328 A^0 from 1 mw He–Ne laser is incident on the SI–GaAs sample. The incident light is chopped using an electromechanical chopper at frequency about 1 Hz, so that optical pulses of long duration (about 600 msec) can be obtained. The neutral density filters (NDF) of different attenuation coefficient are used for variation of photon flux.

The DC electric field is applied between two AuGeNi ohmic contacts situated on the surface of the semi–insulating GaAs. The DC voltage from –110 volt to +110 volt can be applied from Keithley model 236 source measure unit (SMU). This Keithley model 236 SMU instrument sources voltage while measuring current or sources current while measuring voltage

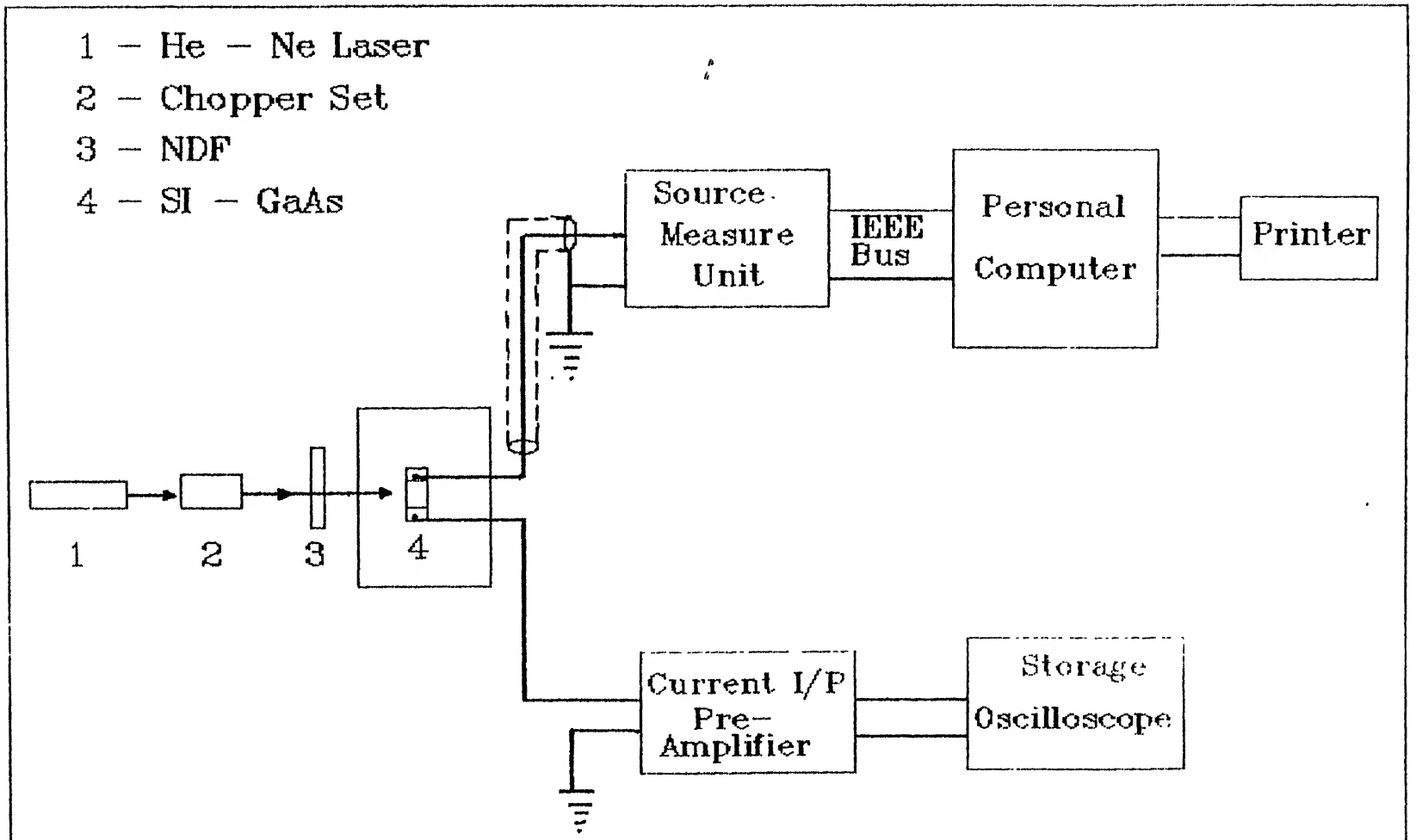

Fig 3.1: Experimental Set-Up Block Diagram

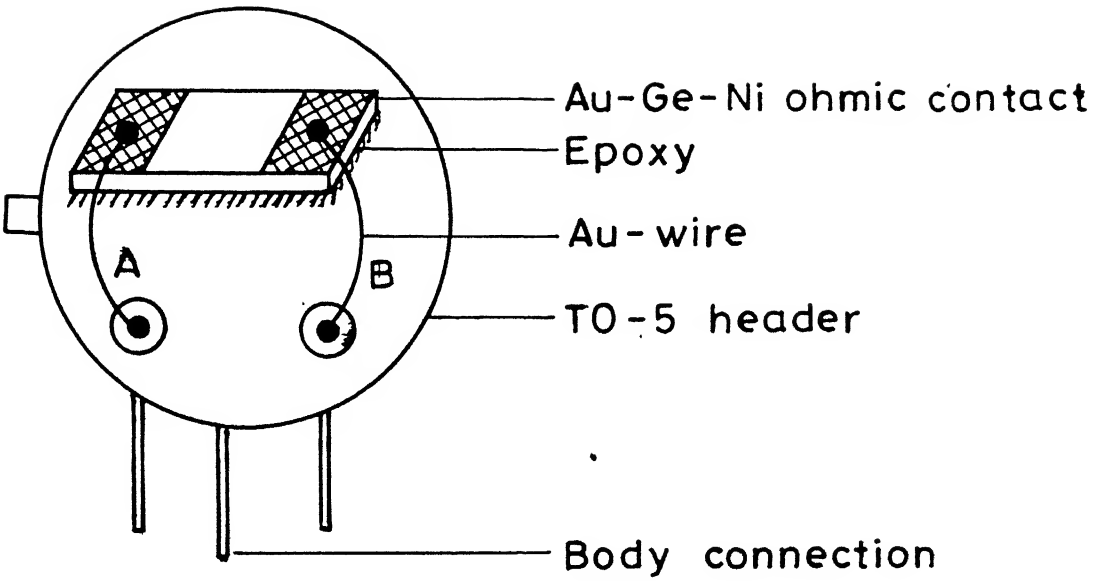

Fig 3.2 Sample specifications and mount details.

On–line data is acquired through IEEE–488 interface. The current through the sample is measured by model 236 SMU. The data acquisition method allows measurement of current data at various times in digital form. The current transients at different DC fields are recorded and stored in the PC. The stored data is then analyzed using various signal processing methods.

For direct observation of current transients and waveforms,the current through the sample is fed to the input of LI–76 pre–amplifier. The LI–76 is current input pre–amplifier with variable gain, which converts current input signal into voltage output signal. This voltage signal is then observed by using storage oscilloscope. By observing these transients it becomes possible to trigger SMU at proper time for recording transients.

ADVANTAGES OF THE DIGITAL APPROACH MEASUREMENTS:

The experimental arrangement described above is based on a digital recording of data. The method of data acquisition allows not only much better control of data measurement, recording and analysis but also reduces some of the problems encountered in an analog approach.

The major advantage of the digital approach is that, the all data is collected in one series of measurements at fixed temperature and varying field. This methood allows recording of entire current transient in single measurement cycle.

This also facilitates fast data acquisition so that, at one fixed field many sets of measurements, and recording of the data can be done. The software designed for averaging, filtering, normalizing of the recorded data helps in noise reduction and analysis of data.

3.2 EXPERIMENTAL DETAILS, OBSERVATIONS AND DISCUSSION.

In this section we describe three different experimental measurements viz. (a) I–V Characteristic measurments (b) Photo–induced current transient measurements (c) Photocurrent transient measurements. The goal of measurements, assumptions made and the experimental conditions are given in the concerned section. During all measurements the sample specification remains the same.

SAMPLE DETAILS: The sample is made from Liquid Encapsulated Czocharalski grown SI– GaAs wafers (Hewlett Packard USA). The contacts made to the sample are AuGeNi alloy (Au= ,Ge= ,Ni=). For making contacts, Au Ge Ni alloy is vacuum evaporated through a metal mask and annealed in flowing H_2 at 450^0 C. The contact geometry is planar. The sample length is about 2–3 mm and the typical distance between the contacts is about 1.5– 2 mm. Two termianls are taken out from contacts by making Au wire bonding to the contacts using conducting epoxy. The sample is mounted on a TO–5 header as shown in fig. 3.2.

MEASUREMENTS OF CURRENT–VOLTAGE CHARACTERISTICS:

INTRODUCTION:

The characterization of the electrical properties of a semi–insulating material is much more difficult and complex than that of a conductive one. The use of the Hall effect for example, is quite difficult due to high impedance, which can lead to poor signal to noise ratio. Also, the conventional methods such as capacitance measurement techniques are not applicable due to high resistivity. In addition, these methods yield results which are characteristic of the bulk of the crystal, while for device applications one is more interested in the properities of the top few micrometers only.

Valuable information about the current transport mechanism in SI–GaAs can be obtained by analysing current voltage (I–V) characteristics. Recent work on I–V characteristics by different invesyigators show different regimes of current conduction as discussed in chapter2 section 2.1. The very existence of so many regimes shows how complex can conduction mechanism be in SI–GaAs. The I–V characteristic also gives information about the critical voltage for the onset of low frequency oscillations. It can be used to obtain information about the static properties of deep level traps inSI–GaAs.

EXPERIMENTAL DETAILS: The I–V characteristics are measured under dark conditions and by illuminating the sample with monochromatic light from 1 mW He–Ne laser at room temperaturer

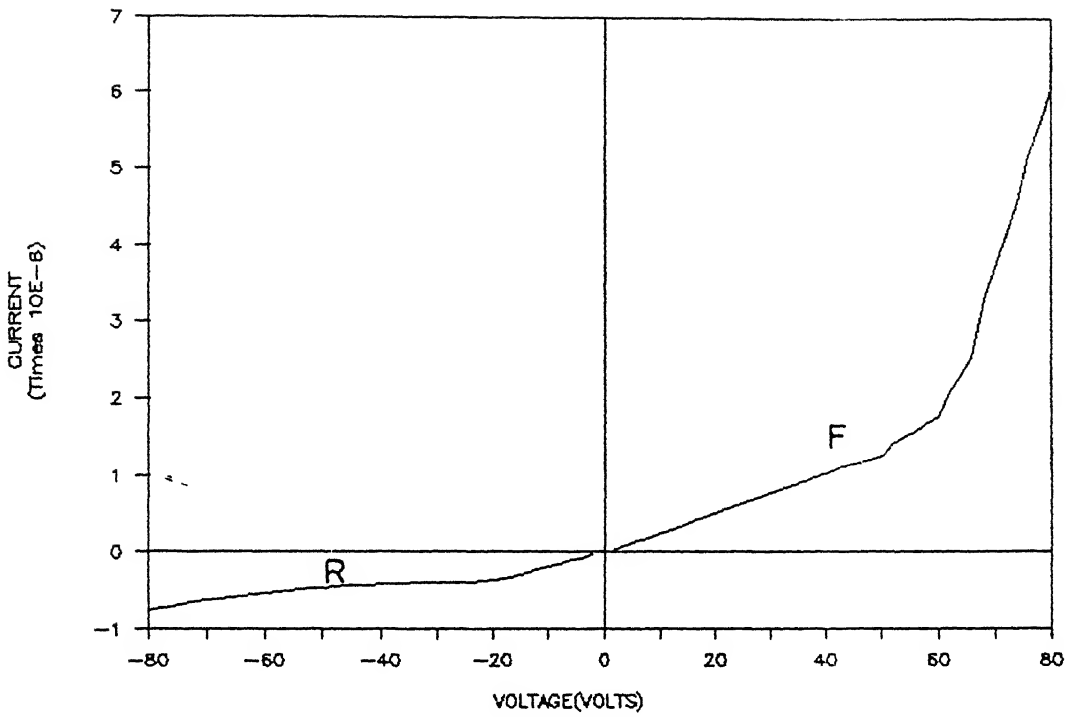

Fig.3.3 Current–voltage characteristics at 300° K in dark (linear scale).

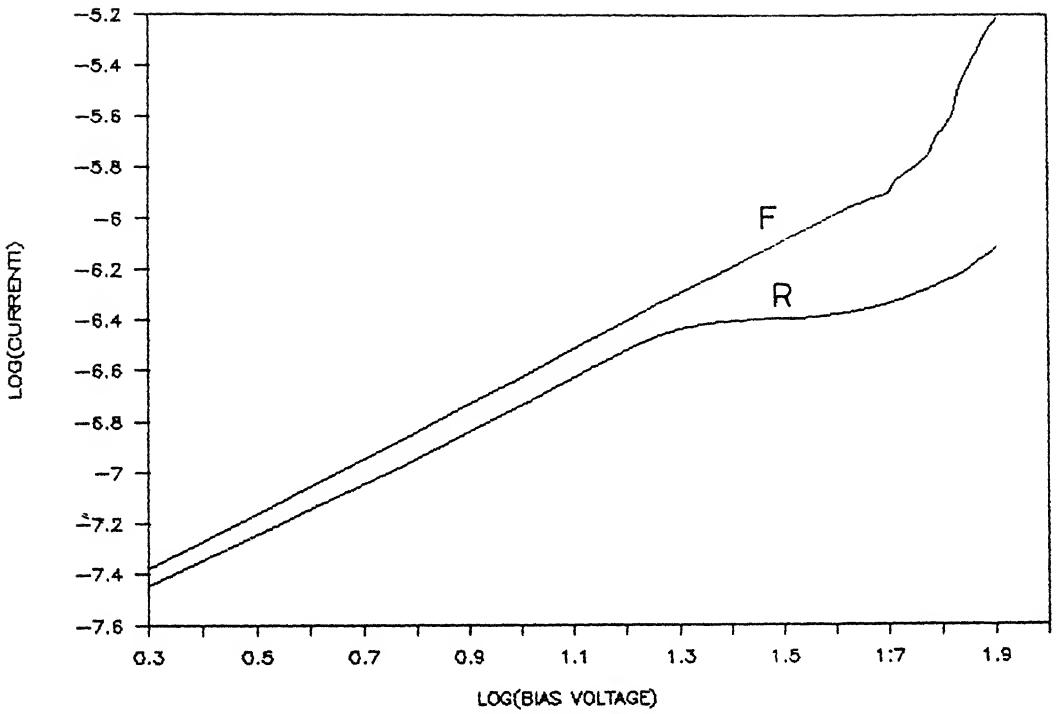

Fig.3.4 Current-Voltage characteristics at 300°K in dark (Logarithmic scale).

in the voltage range 0 to 80 volt (corresponding to fields 0 to 400 V/cm). We also measured I–V curve with different polarity of contact terminals. The fig.3.3 shows linear I–V plot while the fig.3.4 is the logarithmic plot of the I–V curve in dark conditions. The curves F and R are for dfferent polarity of the sample. For simplicity, the curve F is for $A^{+}B^{-}$ polarity and curve R is for $A^{-}B^{+}$ polarity, where A and B are the terminals of the sample shown in fig. 3.2. Since I–V curves of the present device resembles a forward and reverse characteristics of a diode, for simplicity we denote the 'Forward'–like curve as F and 'Reverse'–like curve as R.

FORWARD I–V:

OBSERVATIONS AND DISCUSSION:

The low voltage region (V=0 to 40)of the curves F (Fig.3.4) shows linear dependence of current on voltage. This region is the so called ohmic region. When a certain voltage level is reached, the current rapidly increases with a small change in the sample voltage. The voltage at which this transition occurs is called the trap – filled – limit voltage (V_{TFL}). This transition occurs for V_{TFL} equal to about 48 volt.

The theoratical analysis of low voltage characteristics is based on the single carrier injection model developed by Lampert et al[3]. For this analysis the effect of hole conduction current is neglected because the material is assumed to be n–type i.e. $n_0 >> p_0$, and the electron mobility is much greater then the hole mobility. The rapid increase in the measured current ocurring at V_{TFL} is a trap filling effect resulting from the electron lifetime becoming greater then the electron transit time. The value of V_{TFL} contains information on the concentration of the dominant empty traps (or ionised traps) at thermal equilibrium (N_i). According to Lampert and Mark[3] N_i is given by

$$N_i = \frac{2 \epsilon V_{TFL}}{e L^2} \qquad 3.1$$

where ϵ is the material permitivity, e is the electron charge and L is the distance between the contacts.

Using the experimentally obtained value of V_{TFL} in above equation, the value of ionised trap concentration is $N_i = 1.2 \times 10^{10}$ cm^{-3}. From N_i we can obtain the total trap concentration N_t from the relation

$$N_i = \frac{N_t}{1 + g \exp[(E_f - E_t)/kT]} \qquad 3.2$$

where T is the temperature in kelvins, k is the boltzman constant, E_t is the activation energy of the trap, E_f is the fermi energy, and g is the ground state energy of the deep level. For this snalysis we assume the deep level to have a degeneracy of 2.

Using the relations

$$J = \sigma \frac{V}{L} \qquad 3.3$$

$$\sigma = n \mu e \qquad 3.4$$

$$n = N_c \exp[-(E_c - E_f)/kT] \qquad 3.5$$

and using the standard parameters from (40), the value of trap density N_t(EL2) about 2.7×10^{14} cm^{-3} is obtained which is close to the values normally quoted for EL2 in SI GaAs(46). It is generally considered that EL2 exhibits donor–like tendencies in SI–GaAs(47). Therefore in order to make the material semi–insulating, there must be some acceptor like impurities in the material to compensate the donors. These acceptors may be located close to the valance band (e.g. carbon) and play no role other than to provide compensating holes for the trapping centers. Or, they may be located deep in the bandgap (e.g. chromium) and act as both a ccompensating level and a hole

trap.

The model we use for explaining the I–V curve is one trap single carrier. We assume electron injection and existence of electron trap. At low electron injection level, the current follows ohms law because injected carriers are being trapped leaving the current to be carried by the thermally generated carriers. If the donor trap concentrations are large compared to the thermally generated carrier densities, it is possible that a transition will occur in the I–V characteristics at a voltage corresponding to an electron trap–filled limit voltage (V_{ETFL}) which results from the electron lifetime becoming longer than the electron transit time.

REVERSE I–V:

OBSERVATIONS AND DISCUSSION:

The I–V characteristics in the reverse mode (curve R fig. 3.4) shows a linear region upto 125 V/cm and there exist a sublinear region from 125 to 220 V/cm, and again at higher fields we observe an increase of current. The sublinear region is the negative differential conductivity region, where low frequency oscillations are observed.

The low voltage region is the ohmic region and the theoretical analysis of low voltage characteristics is based on single carrier injection model developed by lampert et al[3]. The explanation for this part of I–V curve is similar to as discussed in last section.

In the negative differential conductivity region many investigators have observed low frequency oscillations and gave different models. The frequency oscillations are caused by travelling domain, and the kinetics of domain travel is given by generation – recombination process between deep trap and conduction band states. First time D. C. Northrop et al (1964) & Ridley and Pratt (1965) reported low frequency ooscillations in SI–GaAs. The model proposed by Northrop et al is based on an analysis of dynamic equilibrium of carriers under the influence of an external field and trapping by a defect. They paid attention to the mechanism of extraction of holes by cathode. Sacks and Milnes (1970) theoretically proposed that the kinetics of domain

motion is governed by field enhanced electron capture by deep level EL2 trap. M. Kaminska et al (1982) proposed model in which they relate the LFOs to carriers being trapped and released by the midgap trap EL2. For oscillations to occur , the capture rate increases for hot electron, which is explained in terms of a configurational barrier, which is more easily penetrated by higher energy electrons. H. Gorokin et al (1984) proposed a model based on recapture at the trailing edge of the domain, which moves with the majority carriers and causes LFOs. G. N. Maracas et al (1985) proposed a model based on diffusion of holes for onset of LFOs.

The role of injecting contact with different contact geometry, polarity and contact spacing in the onset of low frequency oscillations is not properly understood. Lusakowski[38] reported that the role of contacts in the LFOs in SI–GaAs. He reported that, the injecting properties of contacts strongly influence the onset of LFOs. Karpiertz et al[37] also studied the crucial role of cathode for onset of LFO. They took a semi–insulating sample with many contacts of different spacing. They measured I–V curves with different pairs of contacts and observed that, for a given cathode, regardless of the anode, the value of I_{cr}(saturation current which also corresponds to the onset of LFO) is always the same, but it is different for different cathodes. This fact indicate that the cathode injecting property plays important role in the onset of oscillatory behaviour. The frequency of oscillations are observed to be function of many parameters such as dc elecric field, intensity of optical illumination, and temperature.

At present there exists no perfect model which explains various oscillatory phenomena in semi–insulating GaAs. For modelling this phenomena it is important to understsnd and study the role of deep level trap, in particular, EL2 deep donor. It is also important to study the dynamic equilibrium between carriers and deep level trap (EL2) in the onset of LFOs. It is imperative to answar questions such as whether the dynamics of generation – recombination process (responsible for domain travel) is governed by the field enhanced electron capture by deep level trap or governed by carrier injection into the material. It is also important to understand whether the oscillatory phenomena is controlled by field or by carrier density or both.

In order to answer such questions we have carried out the current transient

measuremets. Current transients are also useful in understanding the role of dynamic properties of deep level trap in oscillatory phenomena and studying the role of electrical and optical carrier injected in the onset of oscillatory phenomena.

In the present device the I–V curves measured in dark by changing the polarity of the contacts shows different nature. The reverse I–V curve shows a transition from ohmic to sublinear region at about 25 volt. Many authors[29,35,25] reported this region as the so called voltage controlled negative differential conductivity region, where low frequency oscillations are observed. After this region the current starts increasing rapidly for small change in applied voltage. In the present work we did not investigate I–V curve in high field region due to voltage limit. The forward I–V shows an initial ohmic region and at about 48 volt the current increases rapidly for a small change in applied voltage. This voltage corresponds to the trap filled limit. This observed change in I–V may be attributed to the following facts. There could be contact geometrical asymmetry limiting the carrier injection. The other possibility is that, there could be surface state density change near the cathode contact in reverse mode. This is because the defect density is important parameter for observation of negative differential conductivity parameter. It is known that in the high defect density state material the negative differential conductivity smears out. The other possible reason for the observed polarity dependent I–V is that, the present structure is a metal—semi–insulator—metal (M–SI–M) which resembles like two schottky diodes connected back to back through a resistor, so that the observed characteristics may be due to this structure.

I–V CURVE WITH LIGHT ILLUMINATION:

In the present work we studied the current–voltage characteristic by photon flux illumination. The sample is illuminated by monochromatic light from 1 mW He–Ne laser source. The fig.3.5 curve F_L shows I–V characteristic with light incident at room temperature. In the present work we concentrated only on the forward I–V curve to highlight the current transients which are studied in the forward mode. This I–V characteristic shows a ohmic behaviour from 0 to 150 V/cm. The characteristic shows a sublinear region from 150 to 200 V/cm. In the sublinear

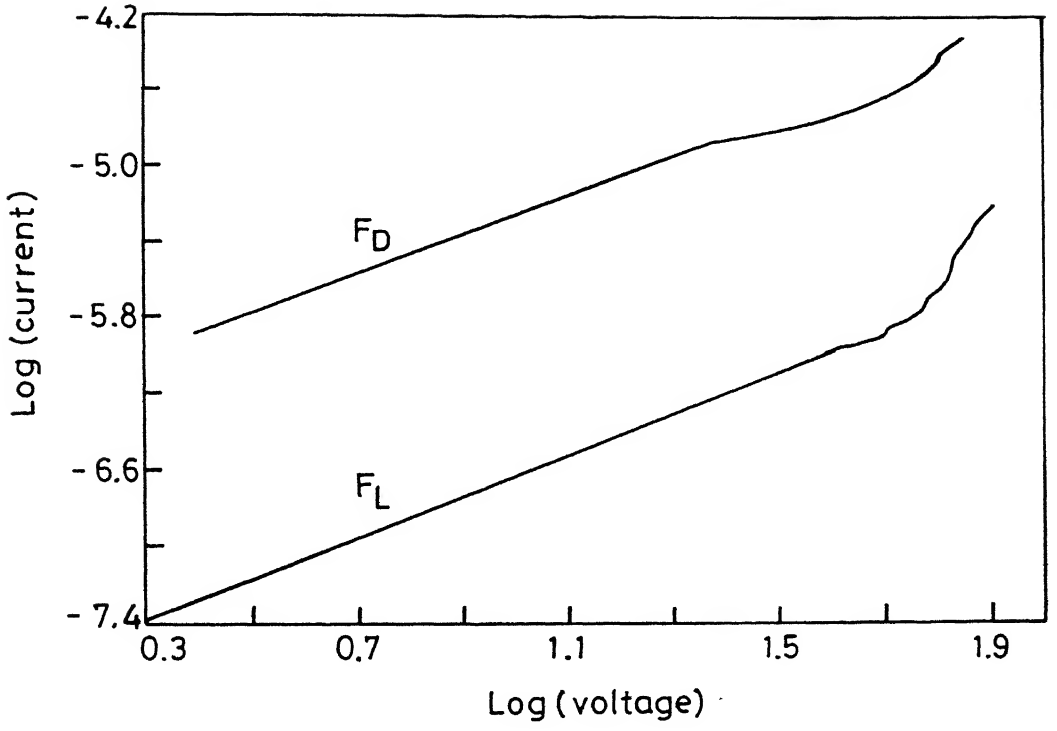

Fig.3.5 Forward mode current–voltage characteristic at 300°K
Curve F_D — in dark conditions.
Curve F_L — with light illumination from 1 mW He–Ne laser

region $I \propto V^{\alpha}$ where α is nearly about 0.5. After this region at about 200 V/cm the current rapidly increases for a small change in the voltage. In the linear ohmic region the transport behaviour is given by single carrier charge injection and trapping as discussed previously. The observation of sublinear region can be accounted for the spreading of recombination front inside the device as the injection level increases[22]. In this region of I–V curve we observe the decaying oscillations in photo–current transients which is discussed fully in section 3.2.2.2. We observe the correlation between the ocurrence of sublinear region in I–V curve and the current oscillatory behaviour. We correlate this relationship in section 3.2.3.

3.2.23 CURRENT TRANSIENT MEASUREMENTS :

The I – V measurements are steady state measurements and are insufficient to give information about, role of dynamic properties of deep level traps in the observation of oscillatory phenomena. The transient study is a good tool for studying the role of dynamic properties of deep level traps in high resistivity material related phenomena. The transient measurement could be either current transient or capacitance transient which are either electrically or optically induced. The choice of methods depend on its suitability to the material and device under study. In particular, the current transient measurement are suited for high resistivity materials. The current transient measurement yeilds information about parameters, such as emission and capture rates, capture cross–section, dependence of rate and cross section on electric field, photon energy and sample temperature.

Among these properties the carrier capture cross section of deep level trap plays important role in SI–GaAs related phenomena. Many investigators have made an attempt to study the variaion of capture cross–section with temperature, photon energy etc. At present there is no direct experimental verification of dc field dependence of capture cross section of deep leveel traps(EL2) in SI–GaAs. One of the initial motivation of this work is to investigate dc field dependence of capture cross section of deep level trap(EL2).

In the present work, we studied the current transient as a function of electric

field. We studied two types of current transients. One is the photo–induced and second is photo–current transient. The time development of current in the material is measured at different applied field. The experimental arrangement used is shown in fig.3.1

The monochromatic light from the He–Ne laser (λ = 6328 A^0, E = 1.95 eV) is incident on SI–GaAs sample . The light is incident in the form of optical pulses using mechanical chopper. The chopper frequency used is about 1 Hz. The light–off and light–on time are such that, the current has sufficient time to acquire steady state value.

To get qualitative idea about the implications of various trap parameters in the onset of oscillatory phenomena, initially, the measurements are carried out in two parts. The frist part corresponds to current transient measurements, where the rate of carrier generation is kept constant and the voltage across the sample is varied. While in second part the current transient measurements are carried out by varying photon flux at fixed applied voltage. In the present work we studied the current transients only in the forward I–V curve polarity of the device, because in the reverse polarity the low frequency oscillations will complicate the situation.

PHOTO–INDUCED CURRENT TRANSIENT MEASUREMENTS :

INTRODUCTION: The photo–induced current transients give information about the carrier emission rate of deep level traps. We studied the dependence of current transient timeconstants on the applied voltage as well as the implication of these timeconstants in the onset of oscillatory behaviour. In this measurement the carriers are generated in the material with photon energy greater than the bandgap energy, which changes the steady state carrier concentration. The optically generated electron – hole pairs are produced only in the top few μm of the substrate, the number of which depends on the illumination intensity. This fact reflects that we are studying the property of top few μm of the substrate.The measured current reflects the time developement of carriers inside the material.

EXPERIMENTAL DETAILS AND OBSERVATIONS: The photo–induced current transient at 25 volt is shown in fig.3.6. The photo current steady state value indicates the carrier density n_{ph} and the value of which depends on the illumination intensity. After the photo current steady state is obtained the light is suddenly swithed off and the time developement of currnt is recorded. The fig.3.6 shows that at time t=0, where the light is swithed off, the current goes below dark value and increases with time and approaches steady state value. This shows that at t=0 the electron concentration aquires a new value $n_0 < n_{ss}$ and approaches steady state value n_{ss} through a non exponential increasing transient.

To analyse the transient for proper interpretation of results, the various signal processing methods are used and are discussed by considering one typical transient for purpose of illustration.

Initially, t = 0 corresponds to the time where light is swithed off. For normalising, the I(t) value is subtracted from I(∞) and then devided by I(∞)–I(o) value. The normalised transient is shown in fig.3.7. fig.3.8 shows log of this data. This log curve appears relatively linear at long times, but it shows the presence of an additional rapidly decaying transient as well for shorter time. As observed by many authors[19,20], that the photo induced current transient is not pure exponential, but it has been observed to be multiexponential. We also observed the similar multiexponential transient shown in fig.3.7. It is seen clearly from fig.3.7 that, there are two transients with initial fast transient for shorter time and then slower transient for longer time.

To estimate the time constant of these two exponentials, best fit method has been used. Initially the slow transient data is best fitted as shown in fig.3.8. The slow transient part is then subtracted from the fast transient exponential and then best fit is employed as shown in fig.3.9. The log of this data shows a straightline fit. We have analysed the data assuming that only two exponentials are present.

The current transients are measured at different field. The above procedure has been employed to find time constants of multiexponentials at different field. The normalised

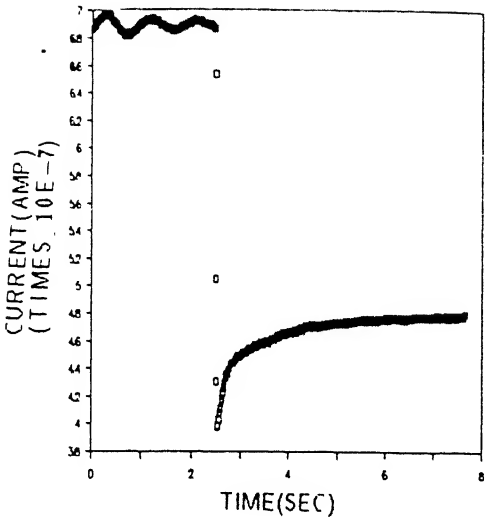

Fig.3.6

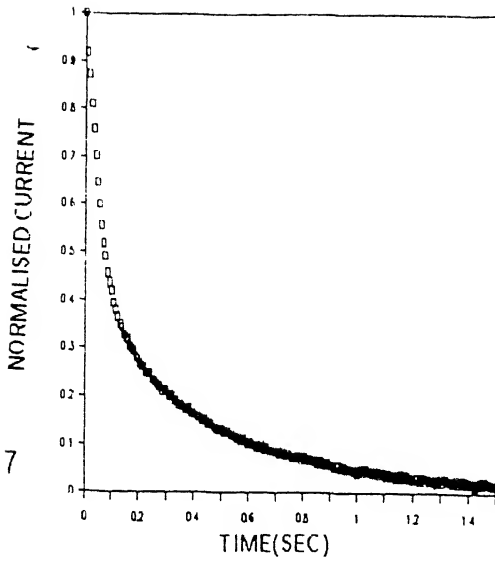

Fig.3.7

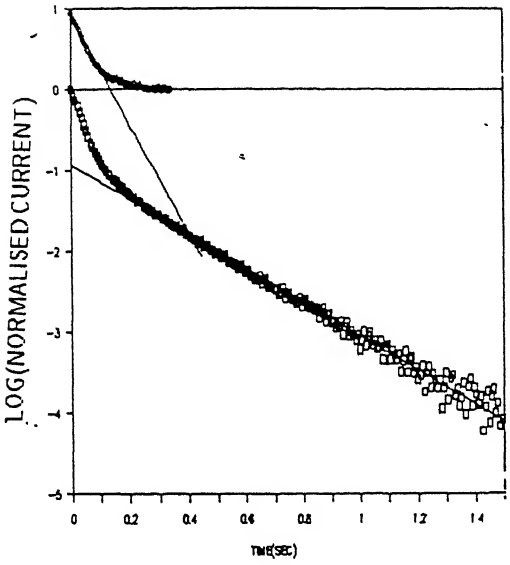

Fig.3.9

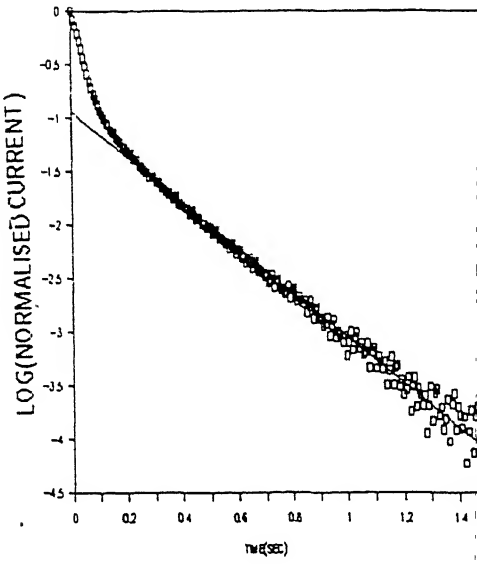

Fig.3.8

Fig.3.6 Recorded photo-induced current transient at E = 125 V/cm (V = 25 volt).

Fig.3.7 Normalised photo-induced current transient at E = 125 V/cm (V = 25 volt).

Fig.3.8 Semi-logarithmic plot of data in fig 3.7.

Fig.3.9 Graph showing slow and fast transient part curve fitting of photo-induced current transient at E = 125 V/cm (V = 25 volt).

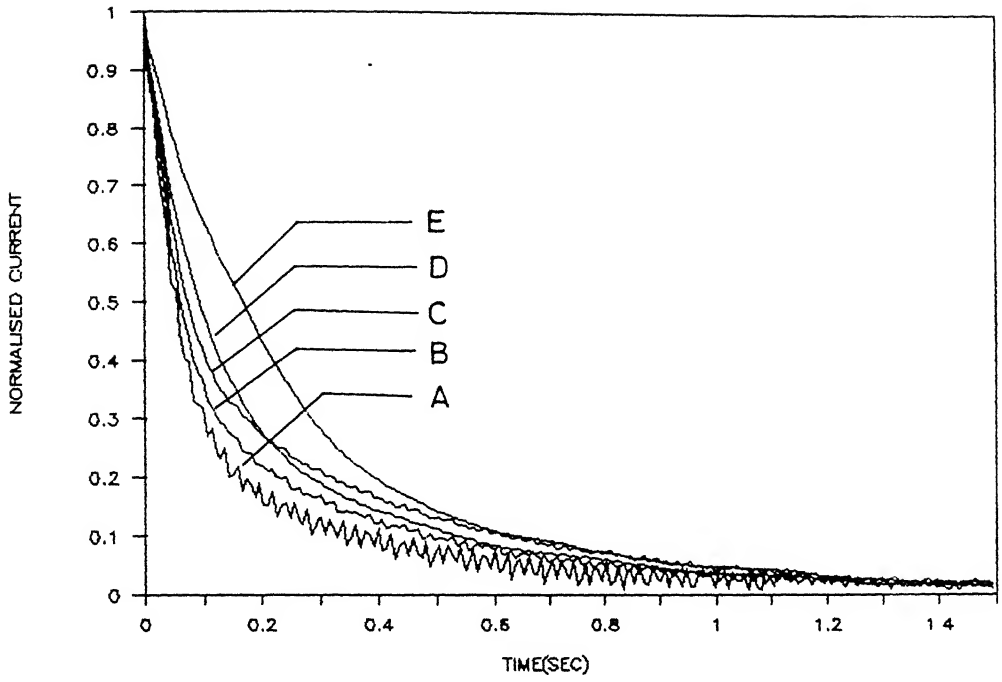

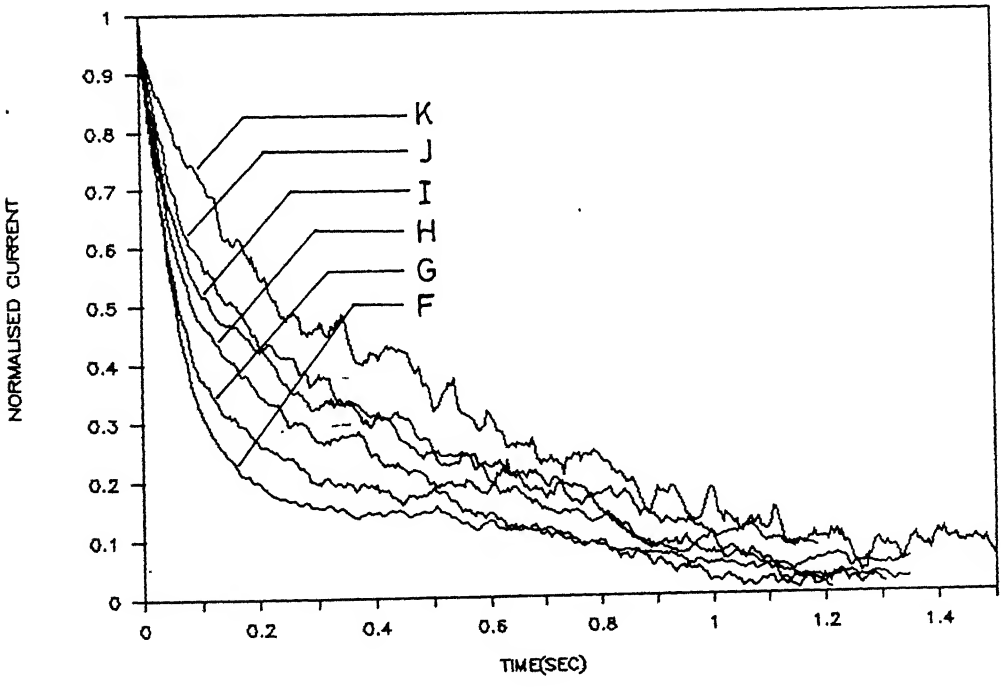

Fig.3.10 Normalised photo-induced current transient at different fields. (A = 75 v/cm, B = 100 v/cm, C = 125 v/cm, D = 150 v/cm, E = 175 v/cm, F = 250 v/cm, G = 275 v/cm, H = 300 v/cm, I = 325 v/cm, J = 350 v/cm, K = 400 v/cm.)

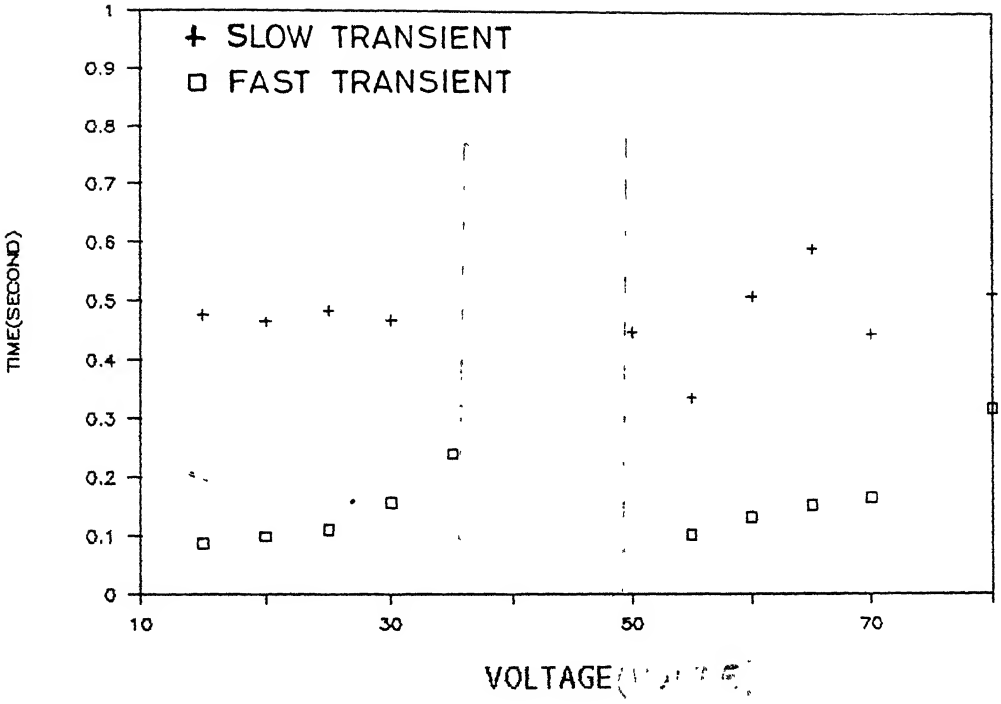

Fig3.11 Plot of fast and slow transient time constant with applied voltage.

current transients at different field are shown in fig.3.10. Fig.3.11 shows the variation of fast and slow current transient time–constants as a function of applied voltage. The value of these time–constants have not been determined for voltages from 35 V to 50 V, because in this region of field the oscillations are riding on the transients.

During the analysis, the data at low voltages showed noise pick–up. This was 50 Hz signal noise which comes from the instrument itself at low current measurments. The data at low voltages < 20 volt has been filtered using a moving averaged filter. The characteristic of this filter is given by the equation

$$I(t_1) = a\, I(t_1) + b\, I(t_2) + c\, I(t_3) + d\, I(t_4) + e\, I(t_5) \qquad 3.1$$

where a = 0.4 , b = 0.2 , c = 0.2 , d = 0.1 , e = 0.1 .

DISCUSSION:

In order to explain the observed behaviour, one way is to assume a number of uniformly distributed electron traplike surface states exist between the contacts, the available density of which is, say N_T. The optically generated electron–hole pairs flood the top few μm of the substrate and the number of which depends on the optical intensity. If the thickness of the substrate is w_s, then N_T occupied surface states at equilibrium during illumination could fully deplete the substrate of N_T/w_s carriers. The population change in N_T due to thermal emission from the surface states after cessation of light pulse is,

$$\Delta N_T = N_{T0}\, e^{-t/\tau} \qquad 3.2$$

N_{T0} depends on n, and the capture and emission cross sections of the surface states. From charge balance considerations,

$$\Delta N_T = n_b\, \Delta w \qquad 3.3$$

where n_b is the carrier concentration in the bulk and Δw is the change in depletion depth. If the current flow through the sample per unit width is I, the voltage applied between the contacts V, and the conductivity of the material σ, then

$$I \alpha V [\sigma (w_s - N_{T0} e^{-t/\tau} / n_b)] \qquad 3.4$$

i.e.

$$I \alpha (V \sigma w_s - V \sigma N_{T0} e^{-t/\tau} / n_b) \qquad 3.5$$

This would produce a current transient which increases with time to a steady state value determined by the dark current level.

Physically, this would correspond to the recovery of the current flow as charge is thermally emitted from the deep level traps which either recombines or trapped or is collected at the contacts.

In the normal PICTS measurements the current transients are measured in a temperature range. These current transients are sampled at two points with the time delays of t1 and t2 and the difference i(t1)–i(t2) plotted as a function of sample temperature. Peaks occur in the spectrum when the rate of emission of carriers from the trap corresponds to the "rate window" set by the chosen values of t1 and t2. The principle, theory and experimental implementation of PICTS are well established[14–19]. In PICTS measurements, which are at low temperature assumes that the dark current level is zero, i.e. there are no thermally generated free carriers present in the material. The present PICT measurements are at room temperature. The thermally generated carriers are available for current conduction, which affects the PICT and makes the problem more complicated.

In the present measurement, PICT are recorded as a function of applied voltage. The transient shows that after light is swithed off, the current goes below dark current value. This is because during light–on time there is significant trapping of electrons by deep level trap EL2, so that, the carrier concentration after light is swithed off attains new equilibrium value

n_0. This new equlibrium value of carrier concentration depends on the trapping rate of electrons by EL2 trap during light–on time. This new equilibrium carrier concentration is less that tha carrier concentration value in dark conditions, resulting in the decrease of current below dark current value after lightis swithed off. The nonexponential behaviour of these transients could be due to superimposition of emission from the deep level traps. The emission timeconstants are of the order of millisecoonds. This fact reflects that, the timeconstants do not correspond to the emission timeconstants of EL2. The EL2 model is not sufficient to explain this behaviour. Published results[20,23,37,38,448,49], suggest existence of other deep level donor traps with activation energies of about 0.56 eV and 0.4 eV. The emission timeconstants may correspond to emission from these deep level traps. Although emission timeconstants do not agree with those of the EL2 emission time constants, the existence of EL2 cannot be ignored. The variation of initial fast transient timeconstant with applied voltage suggest that, this may involve emission from traps with activation energies 0.54eV and 0.4eV. Recently evidence has been furnished[25] that there exist a high field within a very short region ($< 1\,\mu m$) near the anode. It is known that electrons get emitted from the deep dpnpr EL2 in presence of high field by the mechanism of Poole–Frenkel effect[1] with barrier height reduced by field. Hence, the emission observed, in our case, could easily be due to such emission so that the timeconstants observed is less than expected from El2 without any field. In effect, this points to the fact that there is actually Schottky barrier near the anode. The variation of fast timeconstant with voltage is a complicated feature involving more processes, suggesting that there could be competition between the field dependent processes. The slow transient part timeconstant is nearly independent of voltage. This suggest that, it may correspond to pure thermal emission from 0.54 eV trap. This fact reflects that, the the rate of emission of carriers from deep level traps at longer time is nearly exponential and must be field independent. This slow exponential part can be used to define rate window in conventional PICTS measurements to find the trap activation energy.

In photo–induced current transient, we observe an oscillatory current transient from 175 V/cm to 250 V/cm region of field. The initial fast transient time constant shows an

increase with increasing field just before and after the oscillatory regime as caan be seen in fig 3.11. This trend of fast transient time–constant immediately before and after oscillatory region has an information regaarding the mechanissm of onset of photo–induced current transient oscillatory behaviour. From these observations we suggest that, the origin of LFOs can also be empirically studied by trying to understand this phenomena.

3.3.2 PHOTOCURRENT TRANSIENT MEASUREMENTS:

INTRODUCTION: The photo–induced current transient measuremet mostly contains information about the emission rate of deep level traps and may not contain information about capture cross section of traps. In most of the observable phenomena in SI–GaAs the capture cross section of the EL2 trap plays an important role. Many investigators have studied the variation of capture cross section with temperature, photon energy etc. However, there exist no direct experimental observation of field dependence of capture cross section of deep level trap EL2. Photocurrent transients as a function of field is likely to have information regrding variation of capture cross section. This experiment is carried out to understand the role of optical carrier injection in the onset of oscillatory behaviour.

The light–off time is sufficient for the photo–induced current to attain steady state. For this measurment the experimental conditions are same as given for the photo–induced current transient measurement. For simplicity, all the photocurrent transient measurements are carried out only in the forward I–V polarity of the present device, to avoid comlications due to low frequency oscillations, which arise in the reverse I–V polarity.

EXPERIMENTAL DETAILS AND OBSERVATIONS:

The photocurrent transients measured are devided into three different voltage region as low voltage (0–29 volt), high voltage (> 40 volt) and window region (30–40 volt). The fig.3.12 shows the record of current near the positive electrode as a function of time at low and

high voltages. Fig.3.13 shows the normalised current transients at low and high voltage region. The Y abcissa in fig 3.13 represents a normalised current $I_n = \frac{I(t)-I(\infty)}{I(0)-I(\infty)}$. For low voltage region < 20 volt the current I(t) increases very slowly above the I(0) value and attains photo current steady state value. As further voltage is increased from 20 v, there is transition of increasing currnet transient to decreasing current transient at about 23 to 24 volt. The increase of voltage upto 29 volt, the current transient follows a decaying transient.

In the high voltage region > about 50 volt the I(t) initially shows a dip of about few millisecond and then increases and attains a steady state values shown in fig.3.13. In the high voltage region we did not record the behaviour indetail since tha data showed random variation.

The most interesting region of applied voltage is the window region 30 volt to 40 volt. In this window region the transient shows very interesting features. Fig.3.14 shows the record of time developement of current at the positive electrode. The fig.3.15 shows the normalised current transient for the window region voltage. As the voltage across the device is icreased from 29 volt upwards the decaying transient becomes an oscillatory decaying transient, meaning that the oscillations are riding on the transient. With increase in voltage the oscillatory transient goes through second order decay transient to high voltage region transient as shown in fig.3.14.

In this measurement the photon energy is greater than the band gap energy of GaAs. The optical illumination generates electron–hole pairs which depends on the intensity of illumination. All photocurrent transients are measured at same light intensity which means that the carrier generation rate is assumed to be constant.The density of the deep level trap present in the material is assumed to be constant. The only parameter which has been changed during the measurement is the field across the sample.

DISCUSSION:

To explain the observed time developement of current at low voltage which

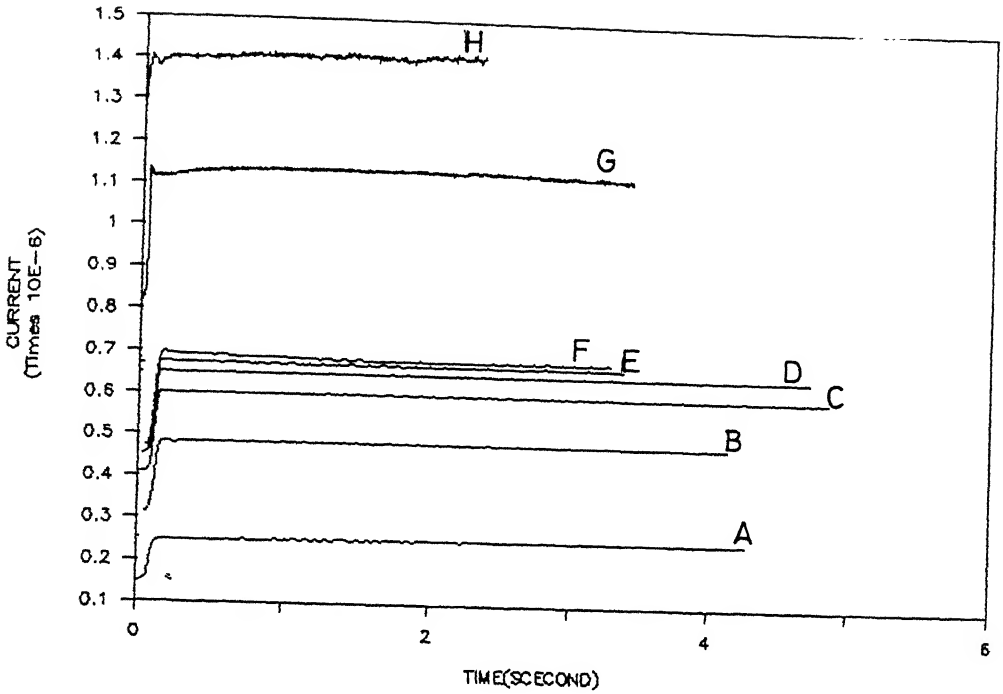

Fig.3.12 Recorded photocurrent transients at low and high field (low field region < 150 v/cm, high field region > 200 v/cm). (A = 50 v/cm, B = 100 v/cm, C = 125 v/cm, D = 135 v/cm, E = 140 v/cm, F = 145 v/cm, G = 225 v/cm, H = 250 v/cm)

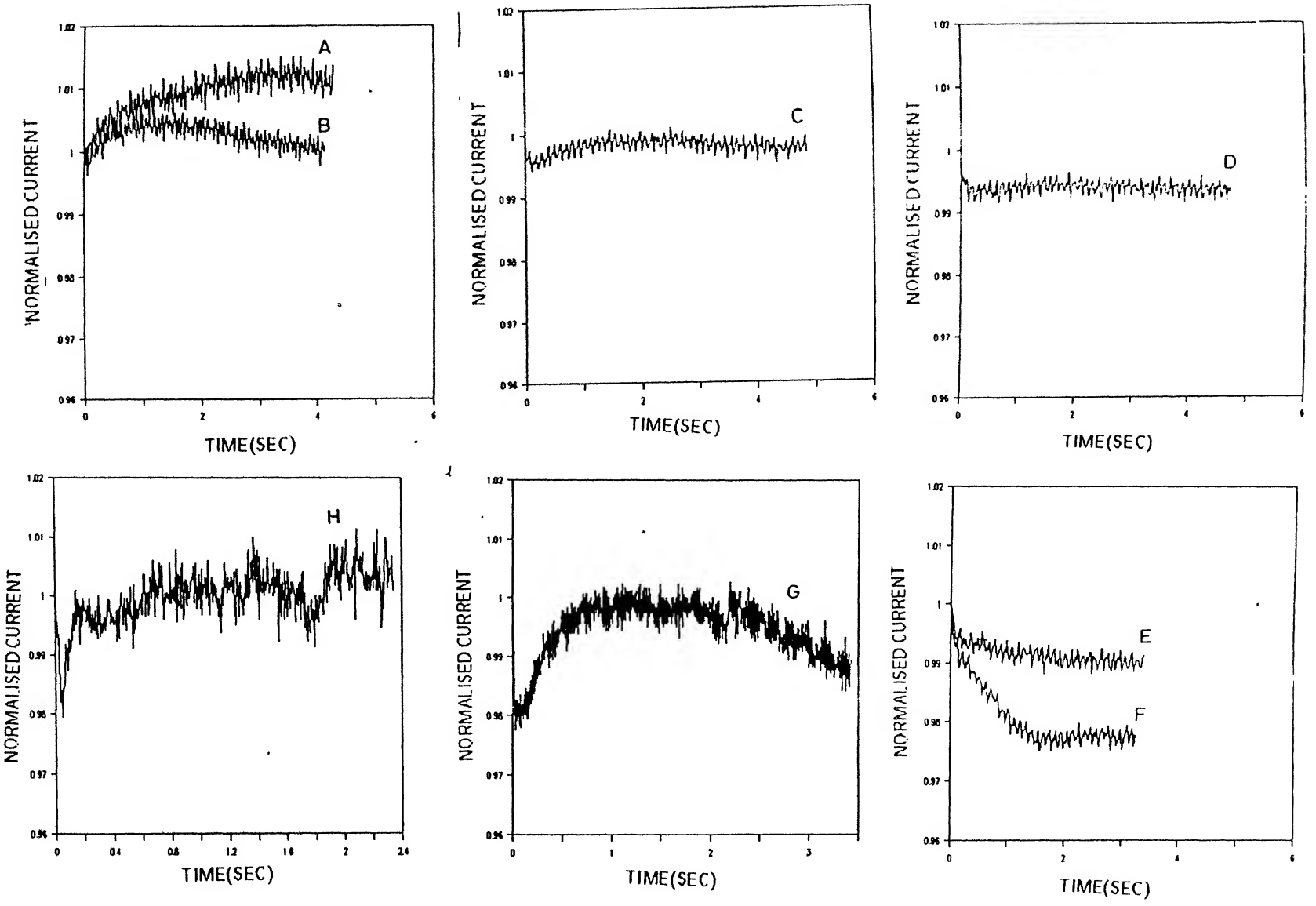

Fig.3.13 Normalised photocurrent transients at low and high field.

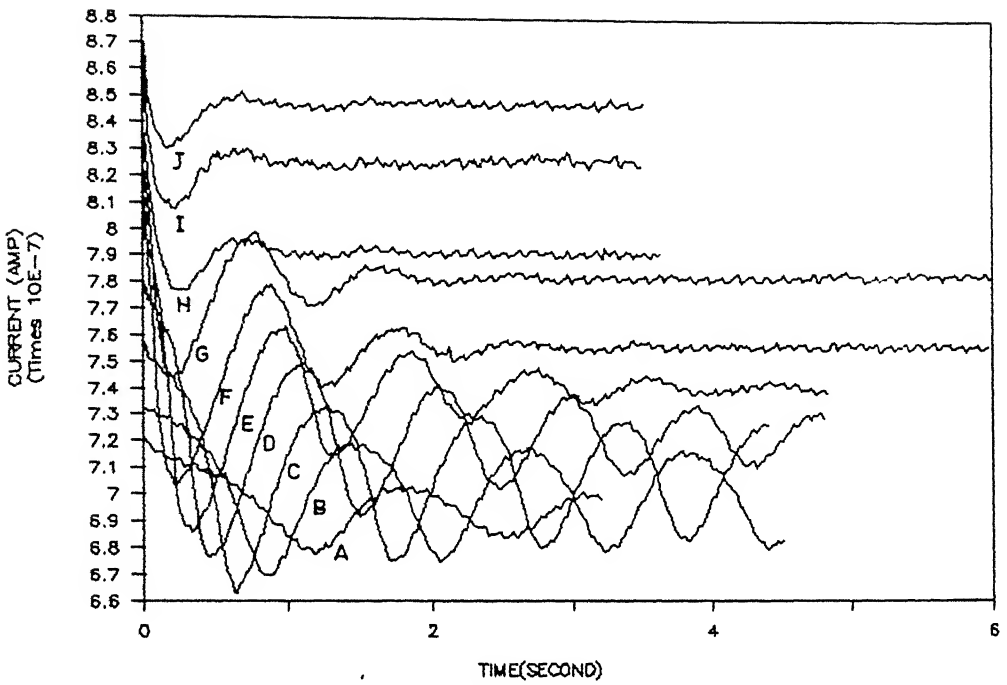

Fig.3.14 Recorded unnormalised photocurrent transient in window region offield. (A=150 v/cm; B=155 v/cm, C=160 v/cm, D=165 v/cm, E=170 v/cm, F=175 v/cm, G=180 v/cm, H=185 v/cm, I=195 v/cm, J=200 v/cm)

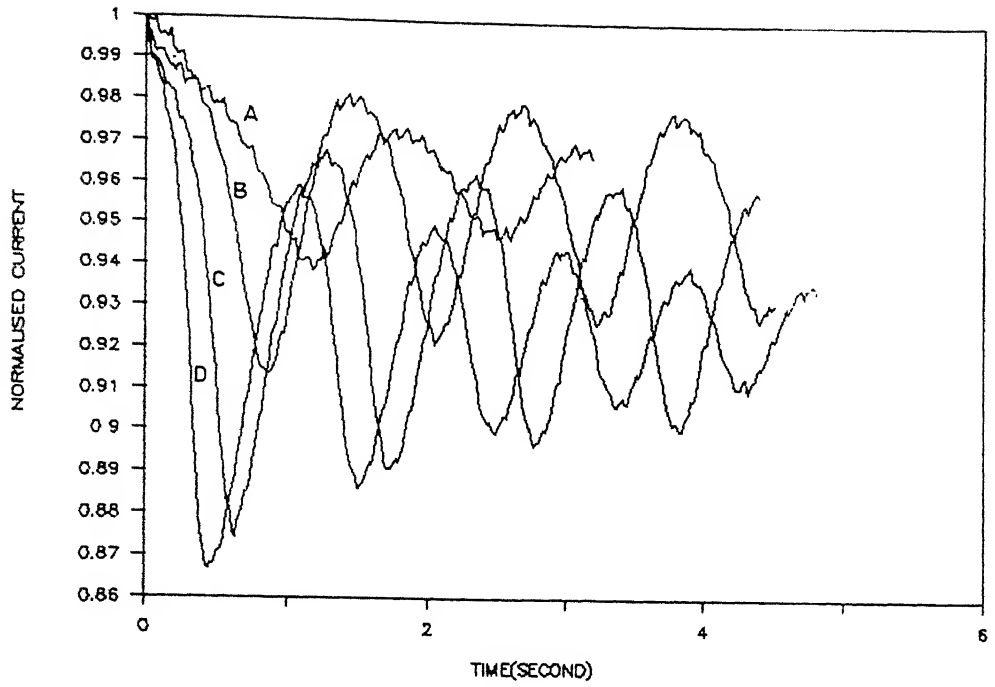

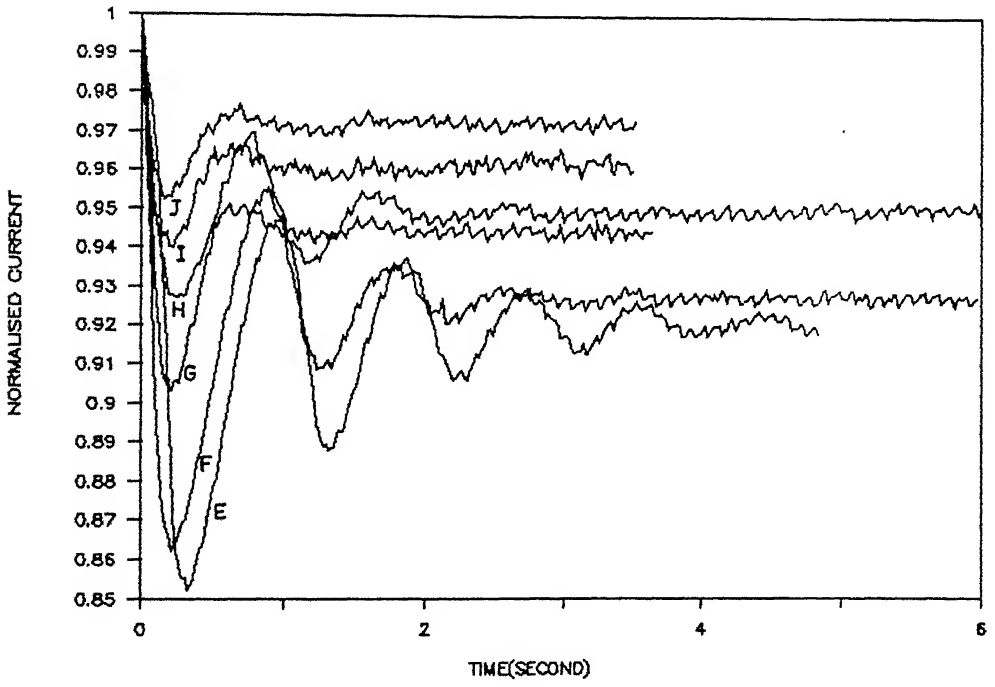

Fig.3.15 Normalised photocurrent window region curves.

CENTRAL LIBRARY
Acc. No. A113492

shows a change from increasing transient to the decaying transient, assume that, at thermal equilibrium and at zero bias there is no significant trapping of carriers from conduction band to the deep level traps. It is also assumed that the current is carried by electrons only and holes do not contribute to the current due to its low mobility. As the voltage is increased the change of transient behaviour at low voltage may be due to field enhanced capture of carriers by deep level trap EL2. This is because as the field is increased the capture cross section of EL2 increases, so that, there exist significent trapping as field is increased. The Field dependence of electron capture coefficient of EL2 has been anticipated in literature[34]. Milnes and Sacks[30] have theoretically shown the field dependence of capture cross section of EL2 trap. According to them the field dependence of electron capture cross section comes from the concept that a negatively charged impurity is surrounded by a potential barrier of height ϕ as shown in fig.2.4. For an electron in the conduction band to be captured by EL2 centre it must either go over the barrier or tunnel through it. The potential barrier ϕ is of the order of 0.08 eV. At low voltage the carriers have no sufficient energy to cross the barrier or tunnel through it so that the capture rate of EL2 is negligible. At low voltages the optically generated carriers will recombine and the thermally generated carriers along with injected electrons from cathode will contribute to the increase of current. As voltage is further increased upto 29 volt, the capture rate of EL2 increases so that more electrons will be trapped which decreases the number of carriers reaching the positive electrode so that the current decreases below I_0 value.

The results shown in fig.3.14 for voltage range 30 to 40 volt represent a complex behaviour. At present there exist no perfect model to explain the observed behaviour. These decaying oscillations on current transients are different from the low frequency oscillations observed in semi–insulating GaAs. The low frequency oscillations are steady state oscillations observed in the negative differential conductivity region due to motion of high field slow travelling domain. The present oscillatory behaviour is observed in the positive differential resistance region of I–V curve brfore the space charge limit (SCL) region. At present the origin of these oscillatory behaviour is not yet clear. In the material with deep impurities when the voltage is incresed above

the ohmic region, the optically injected charge density will decrease the threshold voltage of ohmic to SCL transition[20].

The injected charge carriers from contacts and the optically injected charge carriers may enhance the recombination processes in the device. These recombination process is controlled by charge trapping and detrapping at the deep impurity centre. TAlong with recombination process the charge trapping and detrapping at deep centres can lead to nonlinear fluctuations of carrier density inside the device[47,48]. Without making any assumptions we comment that the decaying oscillatory current behaviour may be due to recombination processes controlled by trapping and detrapping of carriers at deep imputity centers. Similar kind of oscillatory nature has been reported in Si p–i–n devices[47,48]. Goodman[47] accounted the oscillatory behaviour in Si p–i–n structure as periodic fluctuation of carrier concentration between the bounderies and the centre of the 'i' region. Also, Streetman [48] reported that, the oscillations in the Si p–i–n structure, could be due to increase and then decrease of the lifetime as the injection level increases. These oscillatory behaviour is found to depend on, density of deep centers, length of i region, level of illumination, applied bias voltage and position of illumnation. In general these oscillatory behaviour observed in the positive resistance region of I–V curve may be attributed to the formation of recombination wave[49] and its travel caused by trapping and detrapping of carriers by deep level traps. We observe a correlation between these decaying oscillations in current transients and the existence of sublinear region in light on I–V curve. This correlation and its implication in observation of low frequency oscillations in semi–insulating GaAs is dicussed seperately in next section of this chapter.

In high voltage region we did not record the transient behaviour in detail since tha data showed large seemingly random variation. Ralph and Grischowsky[25] reported the existence of trap enhanced high electric field near anode at large applied voltages. They also reported that this trap enhanced field may be enhanced by optical carrier injection. In support of this argument we say that due to existence of large electric field across anode the optial carriers injected into the material may be swept out towards the contacts so that the current at the

positive electrode shows a dip as shown in fig.3.12. As the voltage is still increased the increase of field across anode is concentrated over a small region near anode so that, the time duration of current dip decreases. At present the detailed picture of this behaviour is not understood and requires detailed study of field pattern accross the device.

3.2.3 CORRELATION BETWEEN THE I–V CHARACTERISTIC AND THE CURRENT TRANSIENT BEHAVIOUR:

Fig.3.5 shows the light–on forward current–voltage characteristic (curve F_L). The initial low voltage region upto 24–25 volt corresponds to a ohmic behaviour. In this region of I–V curve we observe an increasing photocurrent transient demonstrating no significant trapping of carriers. After 24–25 volt where the photocurrent transient showed decreasing nature, the I–V curve F_L deviates from the linear region to a sublinear region. In this sublinear region of I–V curve we observe the decaying oscillations in photocurrent transient. From this we demonstrate that the exisence of sublinear region in the light–on I–V curve corresponds to the onset of osillations in the transient mode. We also observe a correlation between the existence of sublinear region (negative differential conductivity region) in the reverse I–V (curve R fig.3.4) curve and the onset of low frequency oscillations. From these observations we demonstrate that, the negative differential conductivity region may be an extreme case of sublinearity which supports stady state oscillations , whereas, a sublinear region but with positive differential resistance, is the region where one observes decaying oscillations in the current transients. This means that, the degree of sublinearity in the I–V characteristic controls the oscillatory behaviour in general in semi–insulating GaAs. This correlation between sublinearity in I–V characteristic and the oscillatory phenomena provides a major clue in mathematical modelling of such phenomena.

3.2.4 PHOTOCURRENT TRANSIENT MEASUREMENT BY VARYING PHOTON FLUX:

INTRODUCTION: The earlier measurements carried out at constant carrier concentration

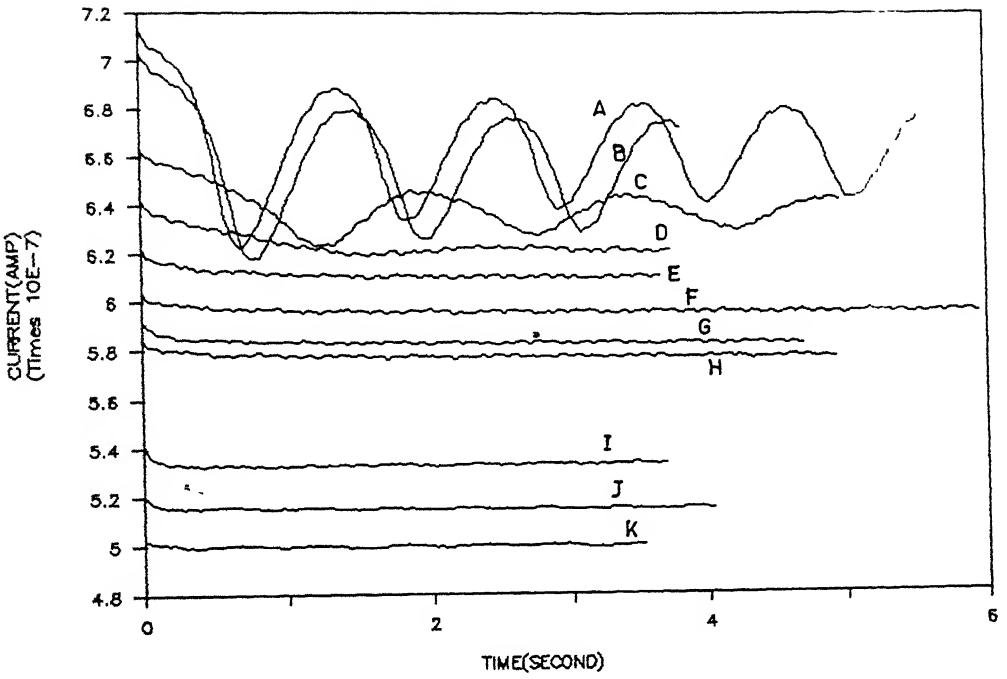

Fig.3.16 Recorded photocurrent transient at 155 v/cm at different photon flux value. (A = 100 %, B = 90.48%, C = 81.87%, D = 74.08%, E = 67.03% F = 60.65%, G = 54.88 % H = 49.65 %, I = 40.93%, J = 13.53%, K = 4.97%.).

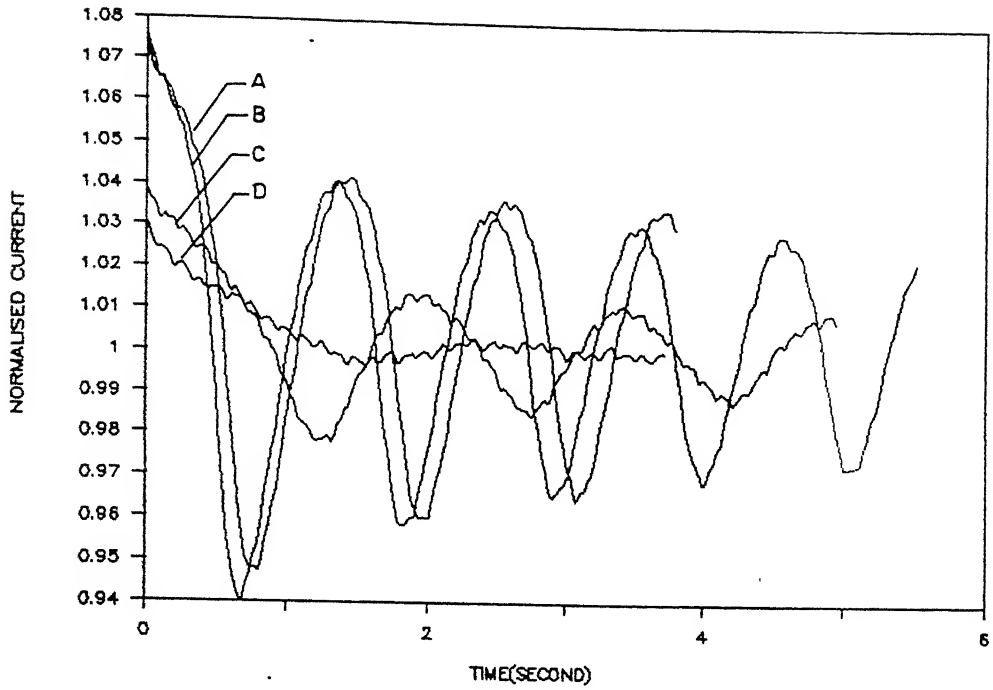

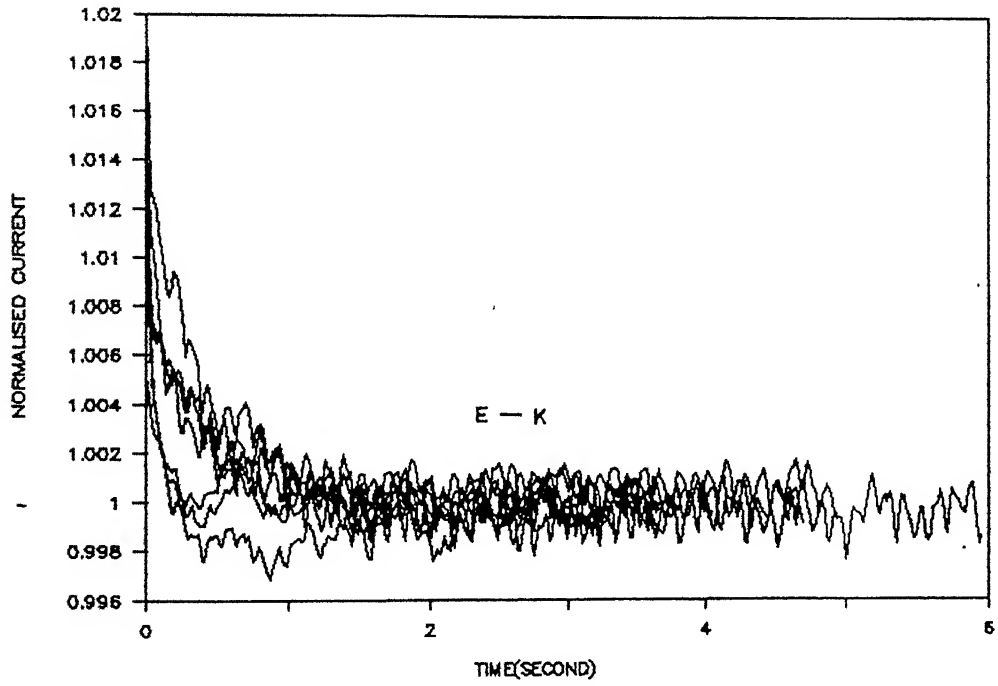

Fig.3.17 Photocurrent transient at different photon flux normalised w r t photon flux at 155 v/cm.

generation and varying dc field shows interesting results. To understand whether these results, in particular, the oscillatory transient behaviour, are controlled by the dc field or by the carrier concentration, we have carried out the measurements by changing the photon flux, which will vary the carrier concentrations generated.

EXPERIMENTAL DETAILS AND OBSERVATIONS: During measurements the photon flux is varied by using the neutral density filters having different attenuation constant. The intensity of light is varied from 100 % to 0.3 % The measurements are carried out at 31 volt, where the oscillations riding on the transient has maximum frequency. Fig.3.16 shows the recorded time developement of current at the anode by varying photon flux. The fig.3.17 shows the transients which are normalised wrt photon flux value.

As a first observation, with reduction in photon flux , the decaying oscillatory transients become simple decaying transient. Fig.3.16 shows that as the photon flux is decreased the oscillation current peak $|I_{osc}|$ decreases. Also the time duration between I_{min} and I_{max} increases. Thus, with decrease of photon flux the slow decaying oscillatory transient becomes a fast decaying oscillatory transient. If photon flux is further decreased then the decaying oscillatory transient becomes a puerly decaying transient.

By normalising all the transient wrt photon flux, one can observe the curve as shown in fig.3.17. The curve shows clearly two features, one oscillatory and one non oscillatory transient; the all the curves fall on each other except for the oscillatory behaviour transients. This shows clearly that the phenomena is purely two processes.

From this measurement one can obsreve that by controlling the carrier generation rate the oscillatory nature can be controlled. These results demonstrate that critical carrier generation rate should be maintained for the onest of the oscillatory phenomena.

Many investigatores[37.38] have demonstrated that for the onset of negative resistence low frequency oscillations in SI–GaAs critical density of carrier injection from cathode is required. Also, in Si p–i–n structure Streetman[48] reported that for onset of the positive

resistence oscillatory nature, critical free carrier density is required in the 'i' region.

Thus, from this experiment we demostrate that, the critical parameter for the onset of oscillatory phenomena in the photocurrent transient is the density of carrier injected into the device.

CHAPTER 4

SUMMARY AND CONCLUSIONS

The present report involves experimental studies of current transport mechanism, and investigations into the role of electrical and optical carrier injection in oscillatory conductance and defect related phenomena in semi–insulating GaAs. Current–voltage (I–V) characteristics of semi–insulating GaAs with injecting ohmic contacts are studied in 0 to 400 V/cm range of dc electric field with changing polarity of contacts in dark and light–on conditions at room temperature. Photo–induced and photocurrent transients are studied with variation of dc field and photon flux.

Current–voltage characteristic of present device with different polarity shows different behaviour. In reverse I–V characteristic we observe a negative differential conductivity region where low frequency oscillations are observed, while in forward I–V characteristic we observe a trap filling effect. From the polarity dependent I–V curve of present device we conclude that the contact injecting property may be playing the major role. We also observe that, the light–on–forward I–V curve shows a sublinear region ($I \alpha V^{\alpha}$, α is about 0.5) in the 145 – 200 V/cm range, while for the same I–V curve in dark we did not observe a sublinear region. We observe that the transport mechanism in the present device is a complex process involving interaction between carrier injection and charge trapping & detrapping at the deep level traps.

Photo–induced current transients are observed to be multiexponential with different time constants. We observe that, these time constants do not correspond to the thermal emission from dominant EL2 deep donor trap. The initial fast transient time constant is observed to depend on applied field while the slow transient time constant is observed to be nearly independent of field. The observed time constants may be due to thermal emission of carriers from deep donor traps with activation energies of about 0.56 eV and 0.4 eV. From the initial field dependent nature of fast transient time constant we conclude that, this may involve either thermal

emission from deep donor traps with activation energies 0.56 eV and 0.4 eV, or may involve Poole–Frenkel emission from EL2 traps near anode due to presence of high field.

We observe that the time developement of photocurrent transient inside the present device shows interesting behaviour such as, i)At low voltage, current transients showed transition from increasing to decaying transient indicating field enhanced trapping of carriers by deep level traps(EL2). ii)In voltage window region the time developement of current showed oscillatory behaviour. iii)The high voltage current transient shows a dip in current for few millisecond, the origin of which is not known at present.

From light–on forward I–V characteristic and the photo–current transients we conclude that the occurence of oscillatory behaviour in current transient and the existence of sublinear region in the light–on forward I–V curve are related. In the reverse I–V curve, we observe a sublinear region, which is negative differential conductivity region where one observes low frequency oscillations. From these observations we conclude that the negative differential conductivity region may be an extreme case of sublinearity which supports steady state current oscillations, whereas, a sublinear region but with positive differential resistence, is the region where one observes decaying oscillations in current transients. These decaying oscillations in current transients may be most probably due to formation of recombination wave[49] and its travel caused by trapping and detrapping of carriers by deep level trap(EL2). From these observations we conclude that the degree of sublinearity in the current–voltage characteristics controls the oscillatory behaviour in general in semi–insulatineg GaAs.

The photo–current transients measured by varying photon flux demonstrate that the carrier density plays important role in the observation of oscillatory behaviour. From this we conclude that the critical parameter for onset of the oscillatory behaviour is the density of carriers inside the device, and not directly electric field as most workers assume.

4.1 FUTURE SCOPE OF PRESENT WORK AND PROBLEM

Semi–insulating GaAs material is still under intensive research due to its increasing importance in frontier technology as a high voltage sub–nanosecond photo–conductive switch material, optically controlled switch material and photo–refractive device apart from its substrate use in GaAs based integrated circuits. The present work suggests many important features which can be studied in future.

1. It is important to study the current–voltage characteristics with different contact geometry and spacing so as to eliminate geometrical parameters for the modelling of oscillatory behaviour in semi–insulating GaAs.

2. The low frequency oscillations and the decaying transient oscillatory behaviour are observed to depend on the degree of sublinearity of I–V curve. At present there exist no mathematical model which correlate these oscillatory nature and one can continue the study to develop mathematical model for these oscillatory phenomena.

3. The present work provides a rich variety of experimental results against which mathematical model of the oscillatory phenomena are to be tested.

4. From the present work of polarity dependent current–voltage characteristics we suggest that one can model the present device as metal—semi–insulator—metal (M–SI–M) structure as two schottky diodes connected back to back through a resistor.

5. In order to investigate the observed features of present work in detail one can continue the study by making temperature as a parameter.

REFERENCES

1. S. M. Sze — Physics of semiconductor devices.
2. D. R. Lamb — Electrical conduction mechanism in thin insulating films.
3. R. K. Willardson, A. C. Beer — Semiconductors and semi–metals vol.6 (Injection phenomena)
4. A. G. Milnes — Deep impurities in semiconductors
5. R. H. Bube — Photo–conductivity of solids.
6. D. K. Schroder — Semiconductor material and device characterisation.
7. T. R. Acoin, R. L. Ross, M. J. Wade, R. O. Sarage — Solid State Technology, P.59,1979
8. J. R. Oliver, R. D. Fairman, R. T. Chen, — Electronic Lett. 17,1981,840
9. H. Winston — Solid state technology, 1983,145
10. R. D. Fairman, R. T. Chen, J. R. Oliver, D. R. Chen — IEEE Trans. on ED–28,2,1981,135
11. G. M. Martin, A. Mitonneau, A. Mircea — Electron lett. 13,1977,191
12. G. M. Martin — Applied physics letters *39*(*9*),1981,*747*.
13. J. C. Bourgoin — J. appl. phys. *64*(9),*1988*,R*65*–R*90*.
14. O. Yoshie, M. Kamihara — Jpn. J. appl. phys. *22*,*1983*,621
15. O. Yoshie, M. Kamihara — Jpn. J. appl. phys. *22*,*1983*,629.
16. J. C. Balland, J. P. Zielinger, M. Tapiero, J. G. Gross, C. Noguet — J.phys.D: appl. phys. *19*,*1986*,57.

J. C. Balland *et al* J.phys.D: appl. phys. *19,1986,*71.

J. C. Abele, R. E. Kremer, J. S. Blackmore

J. appl. phys. *62(6),1987,*2424.

J. C. Abele *et al* J. appl. phys. *62(6),1987,*2432.

S. R. Blight, H. Thomas

J. appl. phys. *65(1),1989,*215.

C. T. Sah *et al* Solid state electronics *13,759,1970.*

J. J. Mares, J. Kristofik, V. Smid, F. Deml

Solid state electronics *31,8,1988,*1309.

M. Eizenberg, Harold J. Hovel

J. appl. phys. *69,4,1991,*2256.

K. Karpinska *et al* Proc. XIX international school of semiconducting compounds, Jaszoowiec 1990.

Stephen E. Ralph, D. Grischowsky

Appl. phys. lett. 59,16,1991,1972–1975.

wu Dingfen *et al* Solid state electronics 29,5,1986,489–494.

J. C. Manifacier, H. K. Henisch

J. appl. phys. 52,8,1981,5195.

J. B. Gunn Solid state electronics 1,1963,88.

D. C. Northrop, P. R. Thorton, K. E. Trezzise

Solid state electronics 7,1964,17.

H. K. Sacks, A. G. Milnes

Int.J. electronics 28,6,1970,565–583.

M. Kaminska, J. M. Parsey, J. Lagowski, H. C. Gatos

Appl. phys. lett. *41,*1982,*989.*

H. Goronkin, G. N. Maracas

Int. Electron. Devices Meeting Proc. *188,1984.*

33. G. N. Maracas, W. Porod, D. A. Johnson, D. K. Ferry, H. Goronkin

Physica 134B, 1985, 276–280.

34. G. N. Maracas, D. A. Johnson, H. Goronkin

Appl. phys. lett. *46, 1985*, 305.

35. G. N. Maracas *et al* — Solid state electronics *32, 12*, 1989, *1887–1893*.

36. J. Lusakowski *et al* — Acta physica polonica A *75, 183, 1988*.

37. K. Karpiertz, J. Lusakowski, W. Knap

Acta physica polonica A75, 1989, 207.

38. J. Lusakowski — Acta physica polonica A *77, 1990*, 391.

39. M. F. Leach, B. K. Ridley

J. Phys. C11, 1978, 2265.

40. D. C. Stoudt, H. K. H. Schoenbach, R. P. Brinkmann, V. K. Laakdawala, G. A. Gerdin

IEEE trans. on ED–*17, 12*, 1990, *2478–2485*.

41. W. T. White, C. G. Dease, M. D. Pocha, G. H. Khanaka

IEEE trans. on ED–*37, 12*, 1990, *2532–2541*.

42. G. M. Loubriel, W. D. Helgson, D. L. McLaughlin, M. W. O''Malley, F.J. Zutavern, A. Rosen

IEEE trans. on ED– *38, 4*, 1991, *692–695*.

43. F. J. Zutavern, G. M. Loubriel, M. W. O''Malley, L.P. Schanwald, D. L. McLaaughlin

IEEE trans. on ED–*38, 4*, 1991, *696–700*.

44. R. P. Brinkmann, K. H. Scoenbach, D. C. Stoudt, V. K. Lakdawala, G. A. Gerdin, M. K. Kennedy — IEEE trans. on ED–*38, 4*, 1991, *701–705*.

45. G. M. Martin, G. Farges, G. Jacob, J. P. Hallais, G. Poibland

J. Appl. Phys. vol.51, 1980, 2840.

46. J. Lagowski, D. G. Lin, H. C. Gatos, J. M. Paarsey, M. Kaminska

Appl. Phys. Lett. 45, 1984, 89.

47. Goodman et al — Phys. Rev. 144, 1966, 588.

48. Streetman et al — Soviet Phys. Solid State 8, 1967, 1580

49. O. V. Konstantinov, V. I. Perel

Sov. Phys. Solid State 6, 2691–2696,1965

50. H. J. Queisser et al

Phys. Rev. Lett. 26,10,1971,551.

Th
621.31937
B379e

A 113497

A113497

LTP-1992-M-BHE-EXP.